VOL. 15 No. 1, pp. 1-36 JULY 1953

Philips Technical Review

DEALING WITH TECHNICAL PROBLEMS
RELATING TO THE PRODUCTS, PROCESSES AND INVESTIGATIONS OF
THE PHILIPS INDUSTRIES

EDITED BY THE RESEARCH LABORATORY OF N.V. PHILIPS' GLOEILAMPENFABRIEKEN, EINDHOVEN, NETHERLANDS

THE 15 MILLION ELECTRON-VOLT LINEAR ELECTRON ACCELERATOR FOR HARWELL

by C. F. BAREFORD *) and M. G. KELLIHER **).

621.384.622.2

A. CHOICE OF PARAMETERS AND GENERAL DESIGN.

B. DETAILED DESCRIPTION OF MAIN COMPONENTS AND CIRCUITS.

C. TESTING AND PERFORMANCE.

This is the second article in the series on linear electron accelerator development published in this Review. Since the appearance of the first article, in which the basic principles of the travelling wave linear accelerator were described by D. W. Fry of A.E.R.E., Harwell, the present 15 MeV machine designed by the Mullard Research Laboratories has been installed at Harwell and is now in full time operation. Used in conjunction with a suitable neutron target, very intense bursts of neutrons are produced and the machine then provides the most intense pulsed neutron source available (so far as is known) anywhere in the world. The large variety of problems that had to be solved in this comparatively novel type of apparatus warranted a detailed treatment, to which more space has been devoted than is usual with the subjects dealt with in this Review.

Introduction

The linear electron accelerator is an instrument of considerable interest to the nuclear physicist. Apart from constituting a comparatively simple and efficient means of producing electrons of energy in the 10 million electron-volt range or higher, the linear accelerator, as was pointed out by Sir John Cockcroft [1]) in 1949, owing to the short duration and the large current in the electron pulse, is valuable as a means of generating short bursts of neutrons for use in "time-of-flight" neutron spectroscopy. This method has gained considerable importance for the investigation of neutron capture or scattering cross-sections of materials used in nuclear reactors.

The first two travelling wave type linear accelerators designed and built by Mullard Research Laboratories were destined mainly for nuclear physics work of this nature at the Atomic Energy Research Establishment at Harwell. The first of these was a 3.5 MeV accelerator similar to the one developed by D. W. Fry and co-workers and described in a previous article in this Review [2]). The second (*fig. 1*), whose installation at Harwell was completed during September 1952 and which is the subject of this article, was designed for an energy of 15 MeV.

Although this machine (as well as the smaller one) was destined for nuclear physics work, the design was influenced by the consideration that linear electron accelerators are likely to assume a very important role as X-ray sources in radio-

*) Formerly with Mullard Research Laboratories, Salfords, England; now Chief Superintendent, Long Range Weapons Establishment, Salisbury, Australia.
**) Mullard Research Laboratories, Salfords, Surrey, England.

[1]) J. D. Cockcroft, Nature **163**, 869, 1949.

[2]) D. W. Fry, Philips tech. Rev. **14**, 1-12, 1952 (No. 1). This article will further be quoted as I.

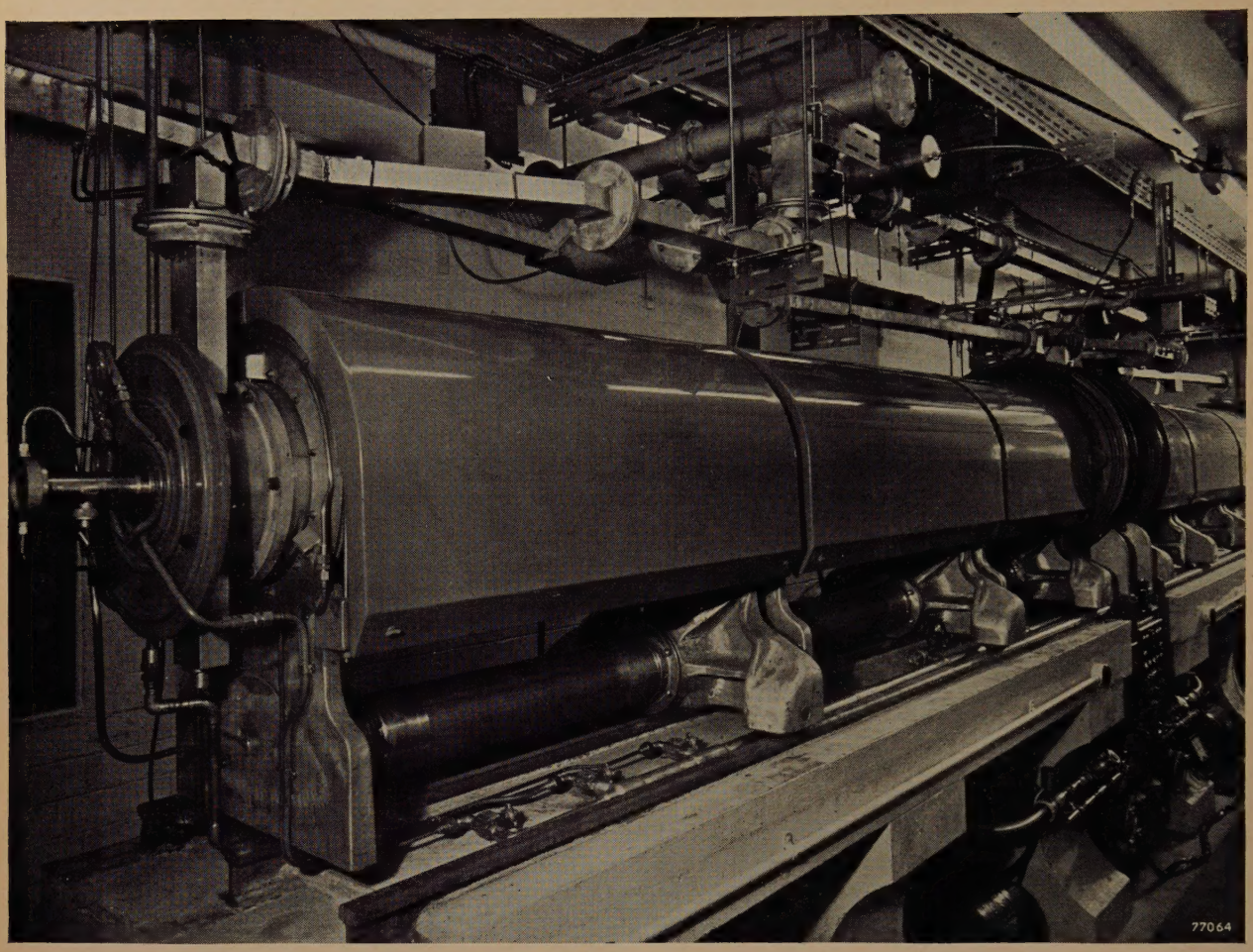

Fig. 1. View of the 15 MeV-accelerator, mounted in concrete shelter at the Atomic Energy Research Establishment, Harwell, as seen from the target end. (This photograph and that of fig. 13*b* are reproduced by permission of the Comptroller of H. M. Stationary Office.)

therapy. In fact, it seems that in the future the most widespread use of the linear accelerator may well be in clinical applications. It will be seen in this description that the 15 MeV accelerator was designed in such a way that it can be used without major modification either as a tool for the nuclear physicist or as a clinical instrument for the radiotherapist.

A. CHOICE OF PARAMETERS AND GENERAL DESIGN

Choice of operating parameters

General

The problem of the design of a linear accelerator for a given purpose depends on a large number of factors, and as in other problems of this nature the final design must inevitably be a compromise. While most of the factors which affect the design have been discussed in I, it will be desirable to recapitulate while discussing the choice of design parameters for the 15 MeV accelerator.

The preliminary data for the design were the following: the performance aimed at was an energy of 15 MeV with 25 mA beam current in the electron pulse; the length of the corrugated waveguide should not greatly exceed 6 m, as this was the space available in the concrete shelter at Harwell in which the machine was to be housed in order to protect personnel from the intense radiation produced; finally the most suitable power source available was a magnetron operating at 3000 Mc/s with 1.8 MW output in the pulse.

In principle a higher operating frequency would be an advantage. This is readily seen from the relationship (valid when the phase velocity is in the region of the velocity of light) between the maximum accelerating field E and the power flux W in the corrugated waveguide through which the

wave and the electrons travel (see I, eq. (2)):

$$E = (480\ W)^{\frac{1}{2}}\ \lambda/\pi a^2, \quad \ldots\ (1)$$

where a is the inner radius of the irises in the corrugated guide. For a given value of a/λ, which is the main parameter of the guide, a higher frequency (shorter wavelength λ) would mean a higher accelerating field per unit power flux (i.e. a higher series impedance of the guide, see I). In the future suitable magnetrons for higher frequencies may become available but at the time when this equipment was designed the pulse powers available at higher frequencies, e.g. 100 kW at 10 000 Mc/s, were much too small.

It was pointed out in I that a choice has to be made between a long guide with low series impedance which is insensitive to frequency changes and a short high impedance guide which is relatively frequency sensitive. This situation is improved by the use of the feedback principle, since the power entering the guide is then higher than the magnetron power and therefore gives a higher energy, with the same impedance, in a given length. It may also be noted that the same electron energy may be achieved with the same length of guide but with a lower impedance (i.e. a less frequency sensitive guide). Even so it may well happen that the frequency sensitivity of the guide will be greater than is compatible with the given stability of the high frequency source. In this case it will be necessary to divide the given total length of guide into two or more independent systems fed from a common source, thus permitting correction of the accumulated phase error at the end of each system.

The decision whether the available length of guide should be subdivided in this way, is complicated by the problem of how much of the maximum accelerating field in the corrugated waveguide can be usefully employed. To emphasize the importance of this point it is necessary to enlarge upon the motion of wave and electron in the waveguide. If it were possible to obtain a high frequency source of very great stability (1 in 10^5) and if it were possible to machine and assemble the corrugated waveguide such that electron and wave velocities are substantially equal at all points of the electron path (machining tolerances $\pm 2\ \mu$ on some dimensions) then all electrons injected at the correct velocity and appropriate phase could travel in the wave crest, i.e. they could be accelerated in the *maximum* axial field. In practice magnetron frequency stability is at best of the order of 1 in 10^4, and it is not economic to machine corrugated waveguides to tolerances closer than $\pm 15\ \mu$. It is therefore clear that the electron must be made to travel in a region of increasing axial field such that changes in guide dimensions or frequency which cause the wave to accelerate more rapidly than the electron, do not cause the electron to move into a region of instability (i.e. of decreasing field *behind* the wave crest). With the guide impedance used up to the present time, it has been found possible to machine and assemble one metre lengths of waveguide such that the phase error of the position of the electrons after traversing one length will not exceed 15°. The accumulation of phase errors due to the mechanical inaccuracy can be avoided by inserting correcting sections of guide at the end of each metre length. Magnetron frequency changes of 1 in 10^4, i.e. 0.3 Mc/s, produce phase errors of the same order of magnitude, so that the total phase error in, for example, a 3 m length would be in the region of 30°. Current practice therefore is to make the electrons lead the wave crest by about 35°, i.e. to make the stable phase for the electrons $\Theta = 55°$. This means that the actual accelerating field on the electron

$$E_z = (480\ W)^{\frac{1}{2}}\ (\lambda/\pi a^2)\ \sin\Theta = (pW)^{\frac{1}{2}} \quad \ldots\ (2)$$

(using the abbreviation $p = 480(\lambda/\pi a^2)^2\ \sin^2\Theta$), will amount to about 80% of the maximum value[3]).

Calculation of performance

For a chosen value of the waveguide parameter a/λ, integration of E_z over the length L of the guide, taking into account the attenuation of power W along the guide, gives the total energy V gained by the electrons. If the beam loading of the accelerator is light, i.e. if the ratio of power transferred to the electron beam to power lost as heat in the walls of the corrugated waveguide is small, the power flux W at any point may be expressed in terms of W_e, the power entering the guide, by

$$W = W_e\ e^{-2\alpha z} \quad \ldots\ (3)$$

where α is the voltage attenuation coefficient expressed in nepers/metre and z is the distance along the guide. Then,

$$V = \int_0^L E_z\,dz = \int_0^L (pW_e)^{\frac{1}{2}}\ e^{-\alpha z}\,dz,$$

[3]) p might be termed the "reduced impedance" of the waveguide: when $\Theta = 90°$, p is equal to the series impedance of the guide.

so that the energy gain per unit length is:

$$\frac{V}{L} = (pW_e)^{\frac{1}{2}} \frac{1-e^{-aL}}{aL}. \quad . \quad . \quad . \quad . \quad (4)$$

In most cases of practical interest, however, the beam loading cannot be neglected. In fact, the ratio of the power absorbed in the beam to that lost in the walls may be of the order of $^1/_4$. A recalculation of (3) and (4) taking into account the power absorbed by the electron beam (beam current I) gives the equations:

$$W^{\frac{1}{2}} = W_e^{\frac{1}{2}} e^{-az} - \frac{Ip^{\frac{1}{2}}}{2a}(1-e^{-az}) \quad . \quad . \quad (5)$$

and

$$\frac{V}{L} = (pW_e)^{\frac{1}{2}} \frac{1-e^{-aL}}{aL} - \frac{Ip}{2a}\left(1 - \frac{1-e^{-aL}}{aL}\right) \quad (6)$$

for the variation of the power flux along the guide and the energy gain per unit length, respectively.

Equations (5) and (6) can be derived in the following way:

The power loss in a length dz of the guide is the sum of the power transferred to the electron beam and the copper loss:

$$dW = -IE_z dz - W(1-e^{-2adz}) = -IE_z\, dz - 2aW dz.$$

Substituting for E_z in terms of W by means of equation (2) and integrating between 0 (where $W = W_e$) and z gives equation (5).

Substituting for W in terms of E_z, again by means of eq. (2), gives:

$$E_z = (pW_e)^{\frac{1}{2}} e^{-az} - \frac{Ip}{2a}(1-e^{-az}),$$

which when integrated over the length L and rearranged, gives equation (6).

From eq. (6) the electron energy to be expected with given values of p, a and L can be computed [4]) provided that the power flux W_e at the beginning of the corrugated guide is known. In an accelerator without feedback this is of course equal to the magnetron power, W_m. In the case where feedback is used (*fig. 2*) W_e is calculated as follows. If it is assumed that there is no loss of power in the feedback bridge itself, but a reduction by a factor k at the input and output feeds to the corrugated guide (see fig. 2), then:

$$W_e = kW_m + k^2W_0,$$

where W_0 is the power flux at the output end of the accelerator. W_0 can be expressed in terms of W_e using equation (5), putting $z = L$. Eliminating W_0 from these two equations gives W_e, and the electron energy can be computed.

Conclusions from the calculations

In this way the accelerator performance to be expected for various designs of corrugated guide was calculated. A few results are illustrated in *figs. 3* and *4*. Fig. 3 is valid for $a/\lambda = 0.2$ and a *single section* waveguide with feedback. Fig. 3*a* shows the variation of electron energy with beam current for various lengths of guide [5]); fig. 3*b* shows the variation of the electron energy with length, for a beam current of 25 mA. In the same diagram is plotted the frequency shift Δf which produces a phase error of 35°.

Figs. 4*a* and *b* provide similar information for a corrugated guide with $a/\lambda = 0.168$ and which consists of *two sections* in series, each with its own feedback loop.

These graphs make it clear that, if the effect of beam loading had been neglected, the error in the estimation of the final electron energy would be 1.5 to 2 MeV.

Considering figs. 3 and 4 in more detail it will be seen that for $a/\lambda = 0.2$ the maximum beam current which can be achieved at 15 MeV in a guide 6 metres long is 12 mA. Alternatively at 25 mA the energy is 14.15 MeV. Under these conditions the permissible frequency change of the magnetron (for a phase shift of 35°) is $\pm$ 0.527 Mc/s. Again by increasing the length, 25 mA at 15 MeV

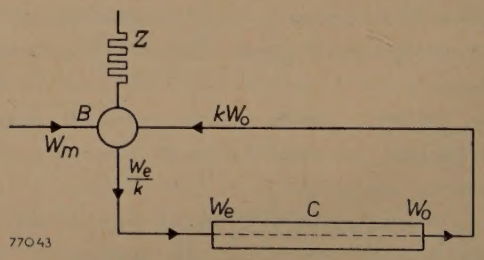

Fig. 2. Power flux in a linear accelerator with feedback. C = corrugated waveguide, B = feedback bridge, Z = dummy load, W_m = power arriving from the magnetron, W_e = "circulating power", W_0 = attenuated power at output end of waveguide.

[4]) The form of eq. (6) is convenient for computation since the function $(1-e^{-x})/x$ has been tabulated by Miller and Rosebrugh, Trans. Roy. Soc. Canada (2) **9**, sect. III, 73-107, 1903, and by G. F. Hardy, Trans. Fac. Actuaries **8**, 57-86, 1918.

[5]) These curves do not represent the variation of energy with beam loading of a practical accelerator. Each point on the curves represents the performance of an individual accelerator in which the corrugated guide has been designed to keep the wave in phase with the electron. Further, it is assumed that the feedback ratio n of the feedback bridge is always maintained at the correct value kW_0/W_m. Since W_0 will vary with the beam loading and n cannot be adjusted during operation, the latter condition will not be fulfilled in a practical case. Therefore, the curve of variation of energy with beam loading in a practical accelerator will be tangential to the appropriate curve in fig. 3*a* at the beam current for which it is designed but at lower and higher currents the electron energy will be less than that indicated in the curve.

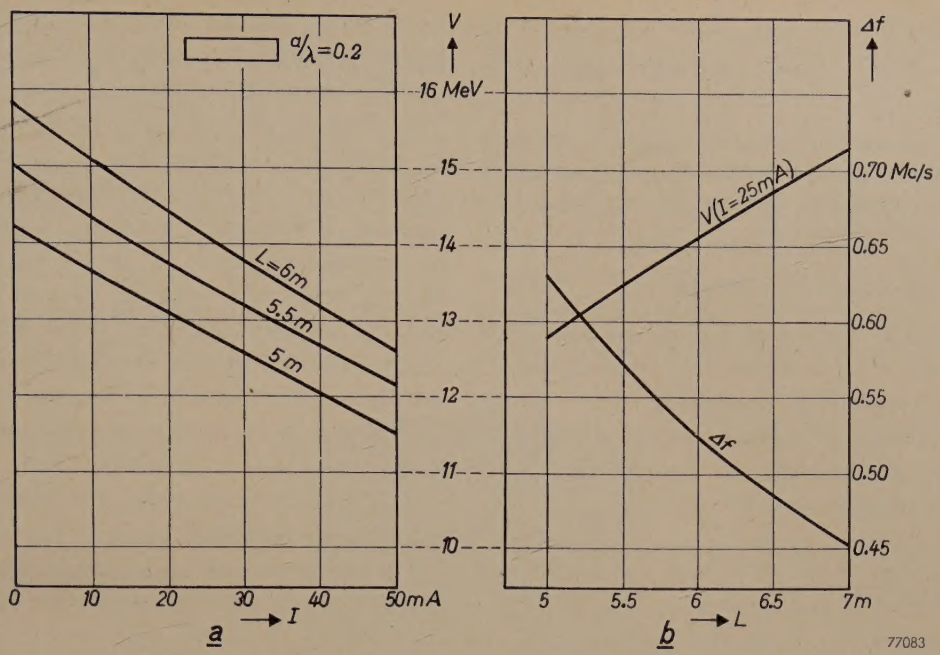

Fig. 3. Predicted performance of linear accelerators with feedback, in *one section* and with waveguide parameter $a/\lambda = 0.2$. Magnetron frequency 3000 Mc/s, magnetron pulse power 1.8 MW; the power loss at each doorknob feed is 5%, or $k = 0.95$.
a) Variation of predicted electron energy V with rated beam current I, for different values of accelerator length L.
b) Predicted energy V for 25 mA rated beam current and magnetron frequency deviation Δf for a phase error of 35°, as functions of accelerator length L.

is obtained with 6.73 metres, but the permissible frequency change is now only ± 0.47 Mc/s. While the frequency sensitivity at 6 metres, with $a/\lambda = 0.2$, is on the borderline, an accelerator could be constructed provided the target performance of either electron energy or beam current is relaxed; on the other hand the target performance can be realised at 6.73 metres but the frequency sensitivity would make the machine difficult to operate over a long period without constant attention.

For $a/\lambda = 0.168$ and the *two section* accelerator it will be seen that a 6 metre length gives 25 mA at 15 MeV with a permissible frequency change of ± 0.62 Mc/s. These were the operating conditions

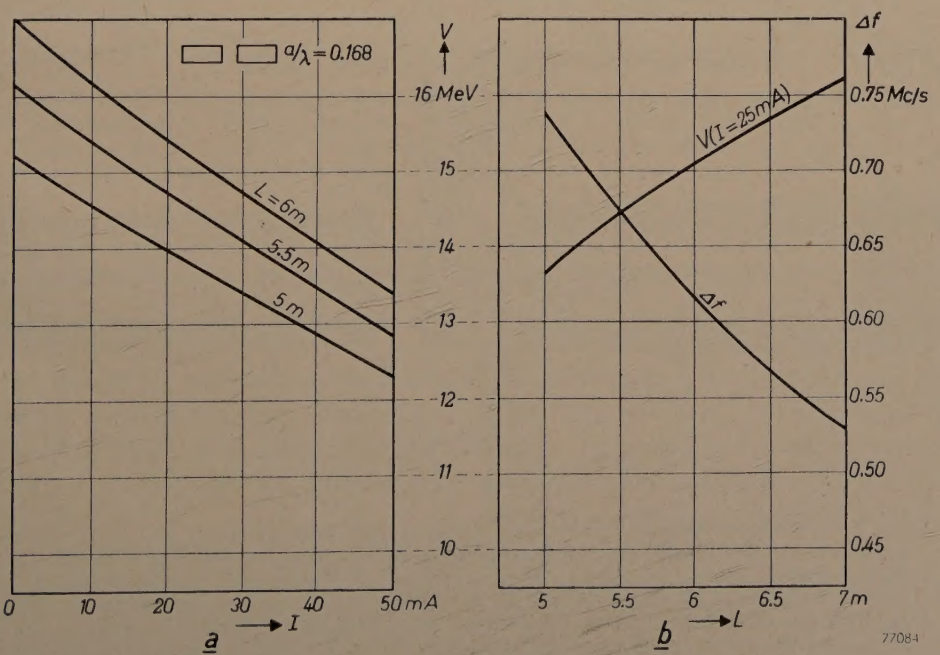

Fig. 4. Same as fig. 3, for linear accelerators with feedback, in *two sections* and with waveguide parameter $a/\lambda = 0.168$.

which were finally adopted. With this choice of a/λ the iris radius of the corrugated guide will be 1.68 cm.

Somewhat more complex conditions apply in the first 30 cm of the guide, where the bunching of the electrons (cf. I) must be accomplished. This has not been taken into account in the above calculations.

Main components of the accelerator

Fig. 5 is a schematic diagram of the operation of the accelerator and shows the relationship of the various waveguide components. *Fig. 6* shows an artist's impression of the layout of the accelerator in the shelter at Harwell; the control desk and general power supply rack are not shown in this drawing.

Referring to figs 5 and 6, a short survey of the main components of the apparatus will be given as an introduction to the detailed description that is to follow.

The high frequency power produced by the magnetron is fed through a rectangular waveguide to a Tee junction (T) where it is divided into two equal parts; the two outputs are fed to the *feedback bridges* B_1 and B_2 associated with the first and second accelerator sections, C_1 and C_2 respectively. The phase of the wave fed to B_2 can be adjusted by means of a *phase shifter* P_0. Power is fed from each feedback bridge to the input of the appropriate corrugated waveguide section (C_1 and C_2) through the "doorknob" feeds D_i. By adjusting P_0 the wave fed to section C_2 is phased precisely to pick up the electron bunches arriving from section C_1. The residual power of the attenuated wave reaching the end of each section is brought via the output doorknob feed D_0 back to the appropriate feedback bridge where it is combined with the incoming power from the magnetron. The phase of the power fed back is controlled by the *phase shifters* P_1 and P_2; a check on the correct phasing is made by monitoring the power levels by means of *waveguide thermocouples* near the input and output feeds.

The *magnetron* (type VX4061) is operated at a power output of 1.8 MW in the pulse, as mentioned above. Its frequency is adjusted by means of a mismatch probe and a line lengthener (ceramic

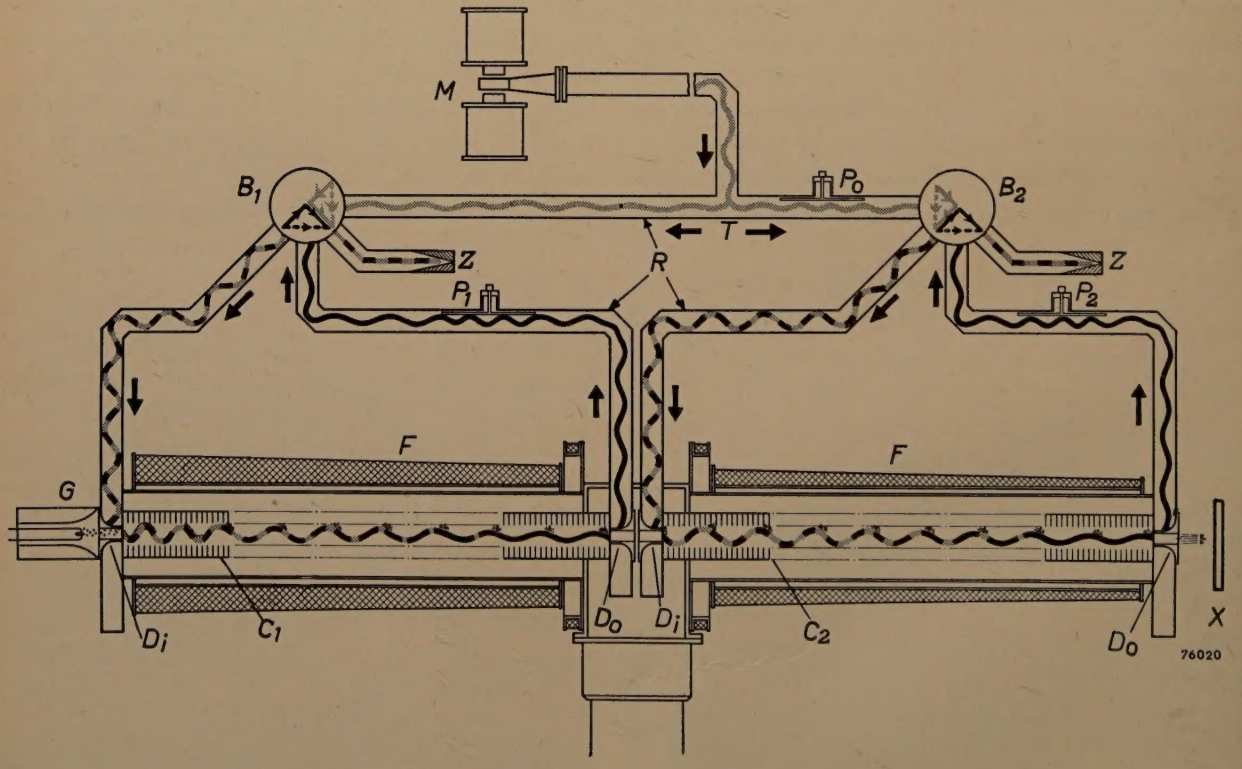

Fig. 5. Schematic diagram of operation of the 15 MeV accelerator. C_1, C_2 = the two sections of the corrugated waveguide, with input and output doorknob feeds D_i and D_0, electron gun G, and focusing coils F. M = magnetron. R = rectangular waveguide system, with dividing Tee T, feedback bridges B_1, B_2, dummy loads Z and phase shifters P_0, P_1, P_2. The power arriving from the magnetron (W_m) is indicated by the grey wave, the attenuated power leaving each accelerator section (W_0) by the black wave; these powers are combined in the feedback bridges and fed to the input doorknob of each accelerator section (black and grey wave). The electrons after being bunched in the first waveguide section travel in a stable phase position somewhat ahead of the wave crest, towards the target X.

wedge phase shifter [6]). The magnetron requires a magnetic field of the order of 0.15 Wb/m² (1500 gauss). This field should be adjustable, as for any given valve there is an individual optimum value. Hence an electromagnet, fed with stabilized current, is preferred to a permanent magnet. The required high frequency power pulses are obtained from the magnetron by feeding to it voltage pulses in the region of 40-50 kV and of 2 μsec duration from the *modulator* (*Mod* in fig. 6). The power in

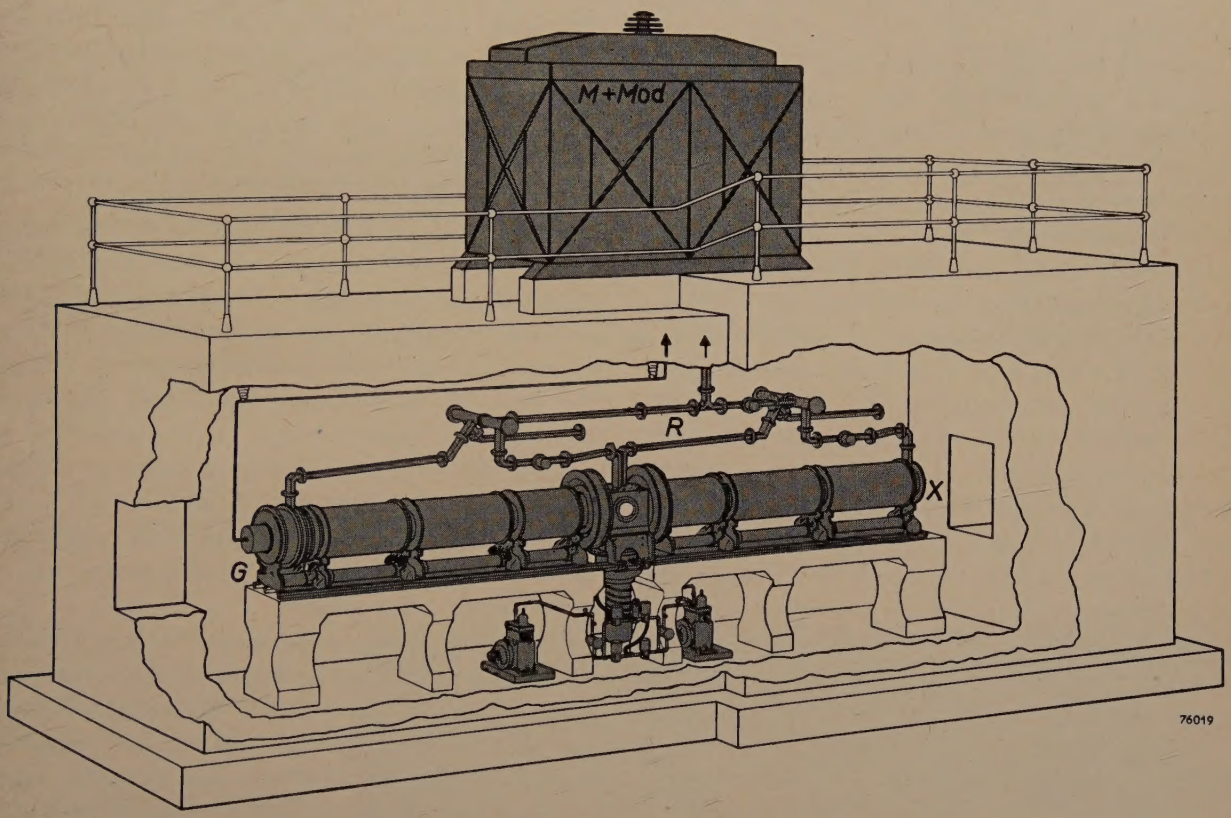

Fig. 6. Artist's view of the layout of the 15 MeV accelerator in the shelter at Harwell. The components are indicated by the same letters as in fig. 5. On top of the shelter are the magnetron *M* and modulator *Mod*. In practice the magnetron has been housed in a separate unit. Note the high-voltage line to the electron gun.

the pulse which the modulator has to deliver depends on the individual magnetron sample, i.e. on the actual efficiency, and may be as large as 5 MW (for an inefficient magnetron).

The modulator design is essentially similar to that of a high power radar modulator and is based on charging a pulse forming network and discharging it through a pulse transformer via an ignitron. It differs, however, in that the condition of freedom from time jitter is of considerably greater importance. In fact, an uncertainty in neutron energy in time-of-flight experiments [7]) is occasioned by uncertainty in the actual time of the modulator pulse, and this error should be small in comparison with other sources of error, for example the duration of the electron pulse. At present the *electron gun* which supplies electrons to the corrugated waveguide is pulsed simultaneously with the magnetron by the modulator. It is possible, however, that shorter electron pulses will be used in the future. It was therefore decided to tolerate a jitter of the main modulator of not more than about 0.1 μsec.

A special circuit involving the use of a "magnetic diode" was developed for stabilization of the gun filament current, as experience with the 3.5 MeV accelerator had indicated that both beam current and X-ray output are very sensitive to small filament current changes.

The considerable defocusing forces acting on the electron beam, especially in the first part of the corrugated guide, are neutralized by the use of

[6]) We cannot in this article enlarge on the details of standard magnetron and waveguide techniques. For such details the reader may refer, for instance, to C. G. Montgomery, R. H. Dicke and E. M. Purcell, Principles of microwave circuits, Mass. Inst. Technol. Radiation Series No. 8, McGraw Hill, New York 1948. See also W. Opechewski, Philips tech. Rev. **10**, 13-25 and 46-54, 1948, and A. E. Pannenborg, Philips Res. Rep. **7**, 131-157, 169-188 and 270-302, 1952.

[7]) T. I. Taylor and W. W. Havens, Nucleonics **5**, 4, Dec. 1949.

focusing coils covering the entire length of the guide and producing an axial magnetic field whose value is just sufficient to constrain the electrons to move in a helix about the corrugated guide axis.

The guide must be evacuated to a pressure lower than 10^{-5} mm Hg, to give a mean free path greater than the length of the electron path (6 m) to avoid loss of beam current by collision with gas molecules. This low pressure will at the same time eliminate the danger of sparking in the corrugated guide, where peak electric fields of the order of 30 kV/cm will be present.

Sparking must also be taken into account in the *rectangular waveguide*. In this case it could be eliminated either by evacuating (to about 10^{-4} mm Hg) or by pressurizing to 2 or 3 atmospheres [8]). While there is little doubt that a pressurized waveguide system would have been very convenient (small leaks could then have been disregarded), it would then have been necessary to develop a waveguide window capable of withstanding a differential pressure of 2 to 3 atmospheres and at the same time of passing up to 1 kW mean power ($^1/_2 \times$ 1.8 MW with a duty cycle of up to 1 : 1000) without undue losses. As a result it was decided to evacuate the whole system right up to the magnetron window.

The *vacuum system* is pumped by a single nine inch diffusion pump whose unbaffled pumping speed is 1500 litres/sec. While it would have been possible to evacuate the corrugated waveguide from one or both ends, the high pumping impedance of an iris loaded structure would give a considerable pressure gradient along the guide. Furthermore it is not improbable that the pressure near the end away from the pump (or the centre) would be too high for satisfactory operation. To avoid these difficulties it was decided to pump the corrugated guide *radially;* it is therefore enclosed in a vacuum envelope, each cell of the guide (see below) being perforated by four holes round its circumference.

To conclude this short survey of the main components and returning once more to fig. 6, it should be noted that the modulator and magnetron have been positioned on top of the concrete shelter. Thus the magnetron and its associated waveguide components have been mounted as close as possible to the accelerator in order to minimize attenuation of power from the magnetron in the rectangular waveguide. At 3000 Mc/s, the power loss in a run of rectangular waveguide, say, 30 feet long, is of the order of 10%. Whereas this is negligible in a radar application it would be quite serious for the satisfactory operation of the accelerator: 10% change in power level would in fact represent a 5% change in peak field and therefore in electron energy.

As the intensity of the radiation from the accelerator is very high (in the region of 2000 röntgen per min at 1 m distance from the target), the walls of the shelter have to be sufficiently thick to reduce the radiation to a reasonable level at all points where personnel may be working continuously. The walls and roof of the shelter have been constructed from barytes concrete, which owing to its high density strongly absorbs X-rays, and the walls are $4\frac{1}{2}$ feet thick in the vicinity of the target.

General mechanical construction

The chief point borne in mind in the mechanical design of the accelerator was that the machine should be easy to assemble. In addition it should be possible to dismantle the equipment for servicing, as required, and subsequently reassemble without the necessity of renewing the initial setting up adjustments. Finally, while it is convenient to support the corrugated waveguide (with its vacuum envelope and focusing coils) from below, it will be essential for medical application of the accelerator to have a clear space below the target end to accommodate the patient.

To satisfy these requirements it was decided to support each metre length of the guide on a separate three-wheeled trolley.The six trolleys are run into position on rails laid on two reinforced concrete tables. Mounted between these two tables is a fixed centre member which carries the diffusion pump (cf. fig. 6). This set-up also allows the trolleys (or only those nearest to the target end) to be supported from above if desired.

Fig. 7 shows the centre member A and the two trolleys T_1 and T_2 adjacent to it. The centre member is machined from an aluminium forging; aluminium was chosen rather than brass for lightness and economy, and as this member forms part of the vacuum envelope a forging is preferred to a casting where the risk of blow holes or porosity exists. The centre member serves also to support the doorknob feeds D associated with the two sections C_1, C_2 of the corrugated guide. The trolleys consist basically of two aluminium end castings which are held apart at the top by the focusing coil former F and at the bottom by a tubular member K. One end of the trolley carries two single flanged wheels and the other end one double flanged centre wheel. Owing to this three-point-support the system will be

[8]) The two possibilities correspond with choosing a point sufficiently high up either to the left or to the right of the minimum of the well known Paschen curve.

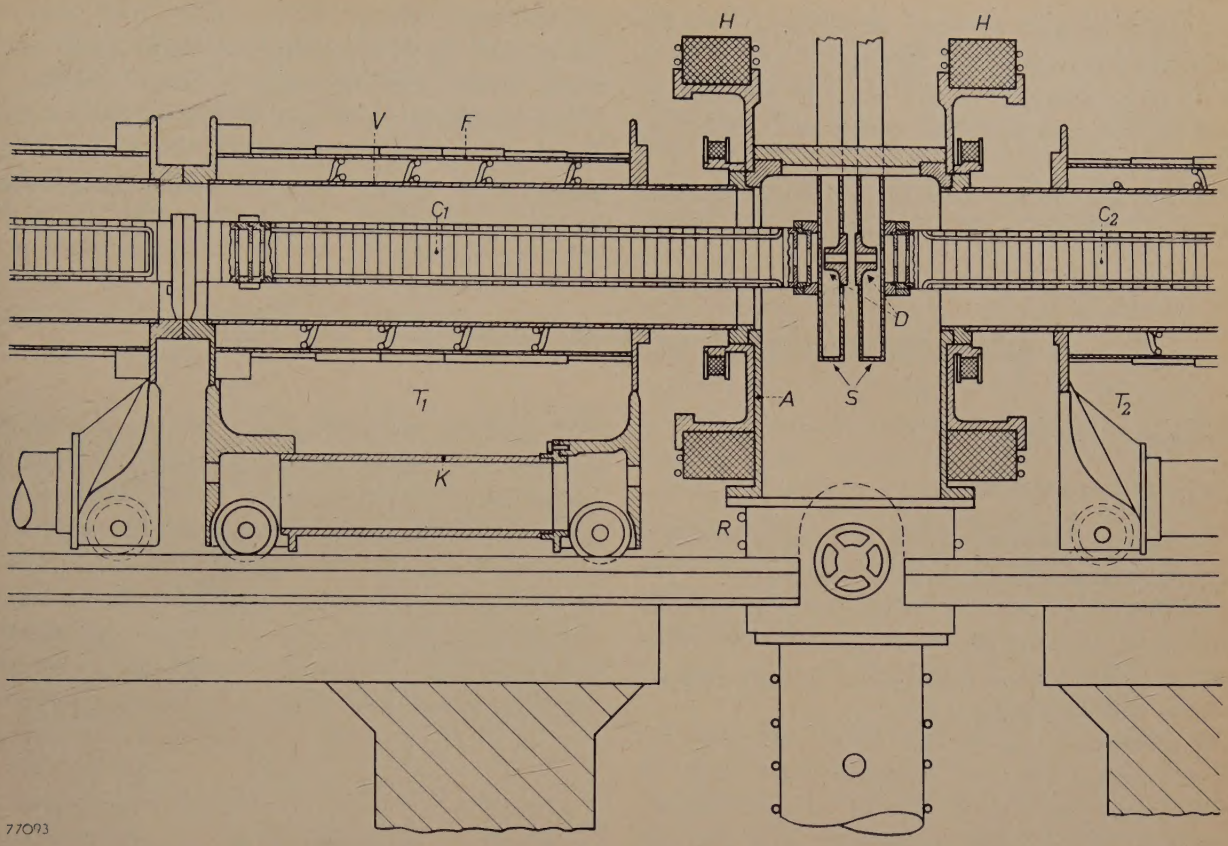

Fig. 7. Centre member A and adjacent trolleys T_1, T_2 of accelerator. F = focusing coil former. K = tubular member. C_1, C_2 = corrugated waveguide sections. V = vacuum envelope. D = doorknob feeds. S = slots in rectangular waveguide. H = Helmholtz coils. O = oil diffusion pump. R = section of envelope with special cooling.

strain-free whatever be the position of the supporting rails. The accuracy required in laying down the three rails, which are rigidly attached to the concrete tables, is determined by the range of the adjustment provided for aligning the trolleys.

Fig. 8 shows a complete trolley prior to connection to the main system. The tubular sections of vacuum envelope consist of $\frac{1}{4}$ inch wall copper tube to which are hard-soldered flanges of strong, nonmagnetic metal ("Delta" bronze, which is much stronger than brass). Each section of vacuum envelope is supported at its flanges inside the focusing coil former by three adjusting screws at each

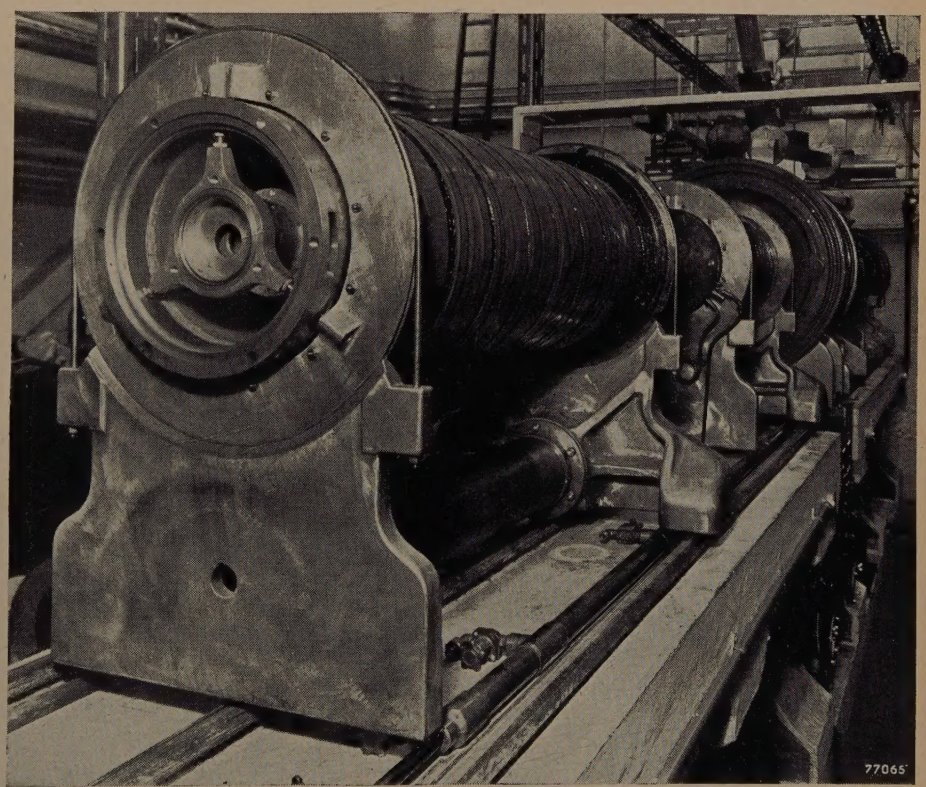

Fig. 8. Complete trolley prior to connection to the main system. The corrugated waveguide supported by a three-legged spider in its vacuum envelope is clearly seen.

end which permit accurate alignment. Similarly each metre section of the corrugated waveguide is in its turn supported in the vacuum envelope at each end by a three-legged spider with adjusting screws.

In this description some of the detailed features of the design have already been mentioned. The second part (B) of this article will continue along these lines, describing the main components listed above and discussing a large variety of detail problems that had to be solved in their development. The third part (C) will deal with the methods of testing and the actual performance of the accelerator.

B. DETAILED DESCRIPTION OF MAIN COMPONENTS AND CIRCUITS

Corrugated waveguide

Mechanical construction

As the successful operation of the accelerator is dependent to a very important extent on the correct performance of the corrugated waveguide, its method of construction required careful consideration in relation to dimensional accuracy and, of course, manufacturing costs.

In particular the surface finish and radio frequency joints between adjacent parts must be such as to give a low value of attenuation, the diameter of the guide must vary with distance along the guide to give the predicted variation of phase velocity [9]) and lastly the inner hole diameter and corrugation pitch must not exhibit irregularities which would give rise to standing waves. The importance of the latter point does not stem from the power loss involved (this amounts to only 0.06 dB for a voltage standing wave ratio of 0.8); the main point is that it severely restricts the tuning range of the magnetron.

The corrugated guide is composed of cells, whose general shape is illustrated in *fig. 9a*. For the major part of the length of the guide a corrugation pitch (length of cells) of 2 cm was chosen as a suitable compromise between the required uniformity of field between corrugations and the copper loss in the dividing walls (cf. I). For the first section of the guide, however, where the electrons must be bunched and where the phase velocity of the wave must vary from 40% to 90% of the velocity of light within a distance of only 30 cm, a smaller pitch is necessary. Thus the first 30 cm of the guide are made up of cells with 1 cm pitch. Next come two special 1 cm cells that serve as a matching section between 1 cm and 2 cm cells. The rest of the guide consists of 2 cm cells. The variation of phase velocity after the first 30 cm guide length is from 90% to 99.8% of the velocity of light at the end of the first three metre length, and then to 99.95% at the target end. The variation of cell diameter (outer diameter of the corrugations) required to produce the variation of phase velocity from 90% to 99.95% of the velocity of light is only 0.2 mm. The cells are spigotted together as shown in fig. 9*b*; a groove is provided at the corner of the male spigot for the insertion of a solder ring.

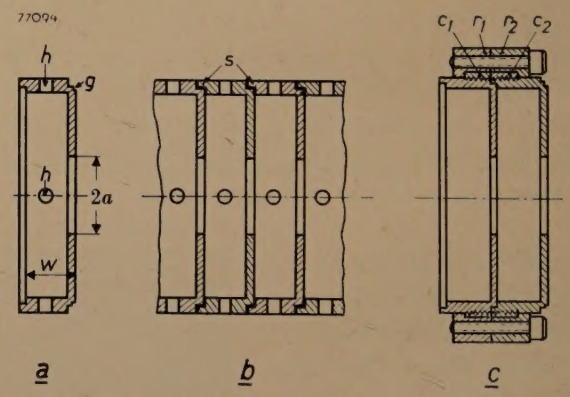

Fig. 9. *a*) One of the 316 cells from which the corrugated guide is composed. Two types of cells are used, viz, of pitch $w = 2$ cm and 1 cm respectively. g = groove for solder ring. h = pumping holes. a = inner iris radius.
b) Two cells showing spigotting action. s = solder fillet.
c) Clamping of two guide sections by rings r_1, r_2 registering on collars c_1, c_2.
The joints shown in (*b*) and (*c*) are important since good radio frequency contact is required.

The method of machining and assembly involved considerable experimental investigation. High conductivity copper strip 5 inch wide and 0.25 inch thick is used as the basic raw material. From this, cold pressings in the shape of a cup (*fig. 10*) are made using a 75 ton press. The pressings are machined to within 0.25 mm of final dimensions. The considerable stresses produced in the material by the cold working must then be relieved in order to avoid the risk of dimensional changes during the subsequent fine machining. The stress relieving is effected by heating to 800 °C in an atmosphere of "mixed gas" (90% N_2, 10% H_2). This process

[9]) The detailed design of the waveguide was carried out by W. Walkinshaw of the Atomic Energy Research Establishment, Harwell.

performs at the same time the function of rendering the copper in the neighbourhood of the surface effectively oxygen free [10]), the importance of which will be evident presently. The cells are then fine machined to tolerances of $\pm 10\ \mu$ at 20 °C on all internal dimensions and on the spigot. It will be appreciated that control of temperature during measurement of the cells is of great importance since an error of 5 °C during the measurement of the guide diameter would suffice to throw the dimension outside tolerance.

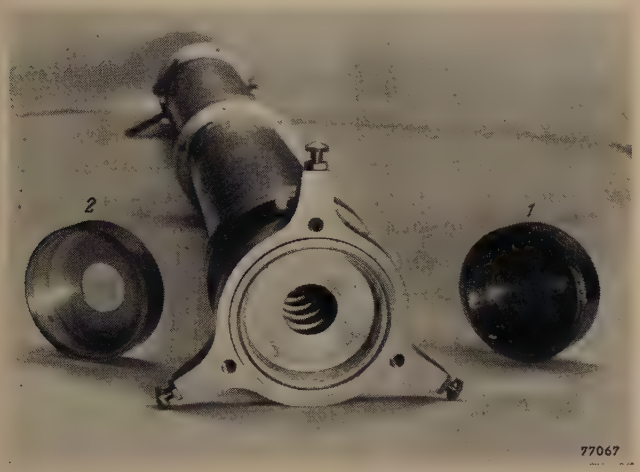

Fig. 10. A length of corrugated guide with centering spider. *1* = cold pressed cup from which a cell (*2*) is machined. Note the pumping holes in *2*.

After machining the cells are degreased and assembled in a stack with copper-silver eutectic solder rings inserted in the grooves provided. The stack is then heated to 780 °C in an atmosphere of pure nitrogen; mixed gas is admitted for a few minutes at the soldering temperature, the hydrogen acting as a flux for cleaning the surface in the soldering process. Finally the guide is cooled slowly in a nitrogen atmosphere. In this way a very satisfactory radio frequency joint is obtained. It should be noted that the surface of the copper in the soldering process must be oxygen free since otherwise the hydrogen flux will tend to cause blisters on the surface of the copper with a consequent serious increase in RF attenuation.

The phase velocity of each section of assembled waveguide is checked by treating the system as a standing wave circuit. A short circuiting plate is placed at one end and RF power at 3000 Mc/s fed to the other; the wavelength and hence the phase velocity is measured by introducing a small loop into one of the pumping holes of each cell in turn and plotting the field pattern. As a result of these measurements of phase velocity, correcting sections of 10 cm length were inserted at four places in the corrugated guide, in the 15 MeV accelerator.

Using the same set-up the attenuation is measured by feeding power into and out of the guide through doorknob transformers and observing the mean power level at points along the guide.

Adjacent lengths of corrugated guide are spigotted and are clamped together by means of a pair of rings, each of which registers on a collar on the end cell as shown in fig. 9*c*. At the end of metres no. 1, 2, 4 and 5 these rings are replaced by the three-legged spiders mentioned earlier and which serve to support and to centre the length of the guide in the vacuum envelope. A length of guide with a spider is shown in fig. 10. The ends of each three metre length are supported by the doorknob transformers.

Water-cooling

At the maximum pulse repetition frequency the power dissipation in the corrugated guide can amount to as much as 300 W per metre length. As the area of contact of the spider adjusting screws with the vacuum envelope is necessarily very small, the only effective points of heat transfer by conduction are at the doorknob feeds. In a few hours running quite high temperatures could therefore be developed in the guide and since a change in mean temperature of only 10 °C produces a 30° phase error between wave and electron, it is necessary to water-cool the guide. This is effected by cooling pipes which have a large area of contact with the guide and which keep the temperature rise within 2 °C.

Since the guide and the vacuum envelope are in effect rigidly clamped together at their ends, any temperature variation of the envelope would cause the guide — which remains at constant temperature — to be in tension or compression, which results in undesirable mechanical strains. (A phase error would also result, but this would be very small since only the length would be affected, where dimensional errors are only 1/20 as critical as on the diameter.) The undesirable effect could be avoided by providing an expansion joint in the vacuum envelope but it is mechanically simpler to pass the cooling water from the guide to a helix soldered to the vacuum envelope so that both are maintained at effectively the same temperature. Before going to waste the water passes to the focusing coil system (to be described presently).

Each metre length of the accelerator has its own water circuit performing this triple cooling function.

[10]) Brit. Pat. Application 23322 of 1952.

Electron gun

The electron gun is a simplified Pierce gun which injects into the corrugated waveguide a substantially parallel stream of electrons. The electrode geometry is shown in *fig. 11a*. A directly heated flat spiral tungsten cathode is situated just inside the apex of a truncated conical focusing electrode. The anode is at earth potential whilst the cathode is pulsed to —45 kV by the main modulator. The cathode structure is supported and insulated by a plate of "toughened" glass.

Experience with the 3.5 MeV accelerator showed that while the average cathode life was in the region of 150 hours, the performance of the accelerator did not give any indication of cathode deterioration until fracture actually occurred. Thus it may well happen that the cathode must be changed in the middle of a long experiment. If cathode replacements required opening-up the whole vacuum system, about two hours would be necessary to re-establish the vacuum after the operation. To avoid this waste of time it was decided to incorporate a vacuum valve between the main accelerator envelope and the electron gun [11]). The valve consists of a slide plate in contact with the flat anode of the gun (fig. 11*b*). Corresponding holes for the passage of electrons and for pumping are drilled in the anode block and slide plate. These holes are in register when the valve is open. When the slide plate is translated to the closed position and pressed on to the anode, the holes in the latter are shut off by "Neoprene" O-rings held in self-retaining grooves in the slide plate. The mechanism for moving and compressing the slide plate is shown and explained in *fig. 12*.

After the cathode has been replaced the gun space is pumped down to about 0.04 mm Hg by one of the rotary pumps of the vacuum system and the valve is then opened slowly. The resultant

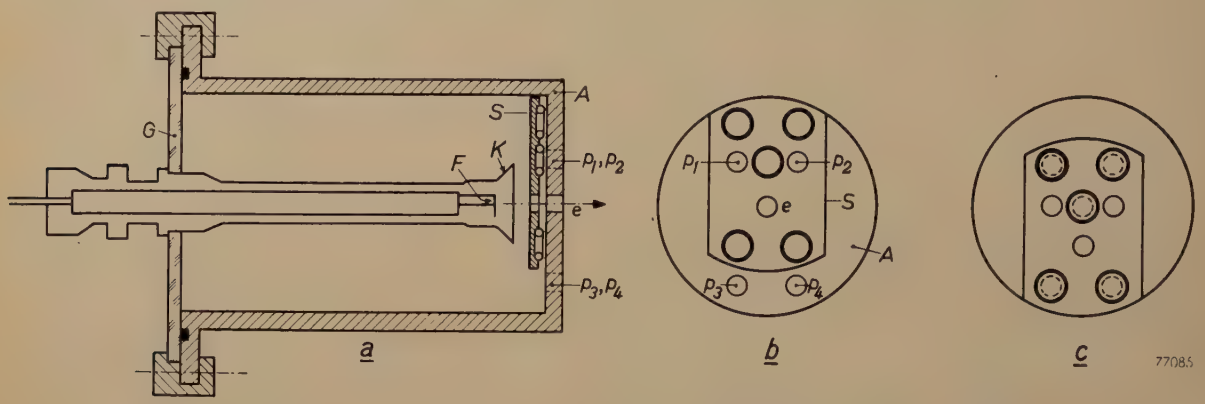

Fig. 11. *a*) The electron gun is of the Pierce type. F = replaceable, directly heated flat spiral tungsten filament. K = focusing electrode. A = flat anode with hole e for the passage of electrons. G = insulating glass plate. S = sliding plate of vacuum valve. *b*) and *c*) Mechanism of vacuum valve. In the open position (*b*) three holes — e for the electrons and p_1, p_2 for pumping — of both anode plate and slide plate are in register; pumping holes p_3, p_4 of the anode are open. In the closed position (*c*) the five holes of the anode plate are shut off by "Neoprene" rings held in self-retaining grooves in the slide plate.

Fig. 12. Electron gun. Through the glass plate supporting and insulating the cathode, the mechanism for actuating the vacuum valve may be seen. The slide plate (with holes) is seen at the far end. The translational movement of the plate is effected by a rack and pinion and the compression by a screw thread. Both movements are controlled by shafts passing through vacuum-tight bearings (Wilson seals) in the gun envelope; the driving knobs are seen at the bottom.

[11]) Brit. Pat. Application 1060 of 1953.

rise in pressure in the main system is very small and the pressure rapidly falls back to its normal value.

It has been stated above that it is desirable to stabilize the gun filament current. Since the cathode is pulsed to 45 kV the problem of stabilization requires special measures. The system adopted is shown in *fig. 13 a* and *b*. A D.C. generator, driven through an insulating shaft by an A.C. motor, feeds the gun filament through an 8 inch diameter cylindrical coil. A magnetic diode (which has a D.C. magnetron characteristic [12])) placed inside and on the axis of the coil examines the field and indicates (by its anode current) whether the field differs from that corresponding to the filament working current. This information is fed via a push-pull amplifier to a servo motor, which drives through suitable gearing and an insulating shaft a variable resistor in the field circuit of the D.C. generator. In this way the filament current can be maintained at its working value. To allow adjustment of the current to lower values, a subsidiary coil surrounding the diode is provided. By passing a current through this coil the field at the magnetic diode is increased and the main current will decrease since the diode will tend to maintain the *total* field at the same value as before.

The only components of the power supply which are at high potential, are the generator, its field resistor and the field coil. A slipping clutch and limit switches are provided to avoid damage to the field resistor if the gun filament should go open or short circuit.

This servo control system has proved very satisfactory in practice and gives a filament current stable to better than $\pm 1\%$.

An alternative and relatively simple method involves feeding the filament through a bifilar choke. Conventional means for stabilization using components at or near earth potential can then be adopted. The choke, however, would have a large capacitance to earth. In the particular case of the accelerator at Harwell it is hoped in the future to pulse the electron gun by a separate modulator having a pulse duration considerably shorter than the 2 μsec employed at present (see page 7). In the interests of economy in this subsidiary modulator it was desirable to keep the capacitance to earth of the gun and its power supply as low as possible.

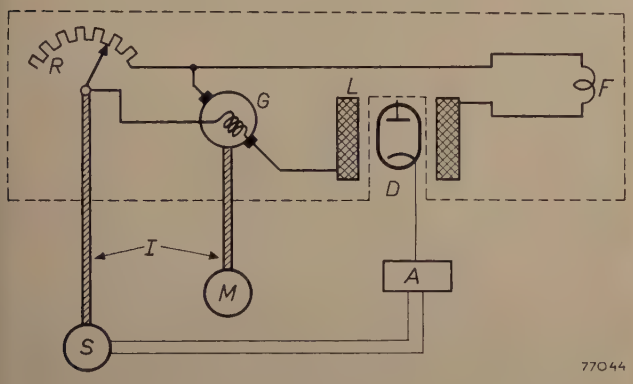

a

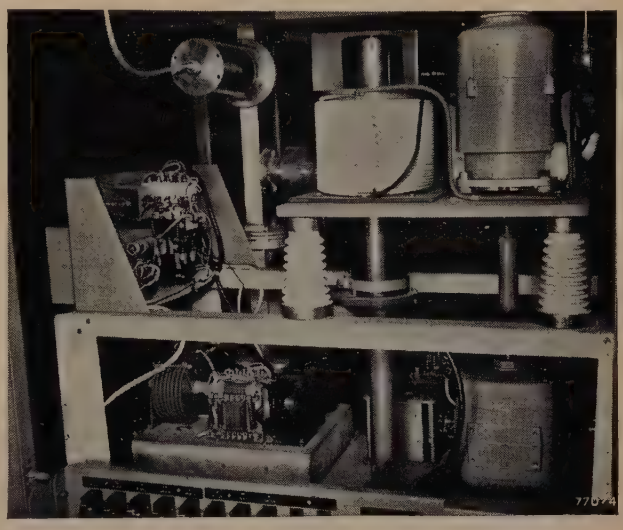

b

Fig. 13. *a*) Circuit for stabilization of the gun filament current. Only the components enclosed in the dotted line are at high potential (—45 kV during the gun pulse). G = D.C. generator driven by motor M. F = gun filament. L = field coil. R = variable resistor. D = magnetic diode measuring the field in the centre of coil L. A = push-pull amplifier. S = servo motor. I = insulating shafts. *b*) Photograph of the stabilizer.

Focusing system

The defocusing forces acting on the electron beam in the corrugated waveguide decrease as the velocity of the electrons approaches the velocity of light (see article I). As a result, the axial magnetic field required for focusing must be highest near the electron gun end of the guide. The calculated value for the 15 MeV accelerator varies between 0.0750 Wb/m² at the gun end to 0.0125 Wb/m² at the target end.

The coil system for producing this focusing field was designed round the use of windings 4 inches long and 10 inches inside diameter, fed by a current in the region of 3 A; the number of turns (and hence the outer diameter of the windings) must vary along the length of the accelerator. The windings are assembled on cylindrical bobbins just under 1 metre long. This subdivision of the

[12]) Cf. H.B.G. Casimir, A magnetron for D.C. voltage amplification, Philips tech. Rev. 8, 361-367, 1946.

coil system makes for easy access to the water-cooling connections of the vacuum envelope at the end of each metre length. To bridge the gap created by the centre member of the accelerator and the diffusion pump (cf. fig. 7) a pair of large Helmholtz coils have been used. To avoid carrying the focusing coils beyond the ends of the accelerator (or alternatively of providing very large coils) in order to maintain the calculated field in the region of the ends, mild steel end plates have been used to provide a local concentration of field.

As the total power dissipation in the focusing coils is in the region of 6 kW, water-cooling has been provided. The cooling pipes are attached to the cylindrical coil formers which constitute the body of the trolley assemblies as shown in figs. 7 and 8. In the region of the gun end, where the power dissipated is considerable, cooling of the cheeks of the coils is also provided. The Helmholtz coils are cooled on one end cheek and on the outer cylindrical surface.

In spite of the water-cooling the mean temperature and hence the resistance of the coils rises during operation and this coupled with mains voltage variations could easily produce a 25% change in focusing field. Stabilization of the coil current was therefore necessary. In this instance it was decided to supply the coils from six independently variable stabilized power units, as experience with the earlier accelerator had indicated that a slightly higher beam current could be obtained by local changes in the focusing field from its predicted value. The six sections of the coil system were chosen such that each power unit supplies approximately the same wattage. This means of course that the coil divisions become progressively longer in the direction of the target; this feature is convenient since it is to be expected that the actual local value of field will be more critical in the low velocity region.

The field stability required was estimated to be in the region of $\pm 5\%$. A magnetic diode circuit was used for the stabilizer units as this was considered to be convenient and economical even though no high voltage problems are involved and the precision achieved is better than required.

Vacuum system

The diffusion pump gives a pressure of 2×10^{-6} mm Hg measured at the top of the centre member of the corrugated guide, under normal running conditions. Although the pumping conditions for the corrugated waveguide are not ideal, owing to the small diameter of the pumping holes in the cells, the actual pressure in the path of the electron beam is probably not greatly in excess of the measured figure and satisfactory operation of the accelerator is achieved provided the pressure, as measured, is not in excess of 4×10^{-6} mm Hg. Pumping conditions for the long rectangular guide with its small cross section are even worse but fortunately the vacuum requirements in this guide are not so stringent. Some pumping of the rectangular guide will occur through the doorknob cones and the corrugated guide. This in itself is undesirable since it tends to increase the pressure in the corrugated guide. Slots have therefore been made in the rectangular guide sections of the doorknob feeds (S in fig. 7). Pumping through these slots provides a satisfactory operational pressure throughout the whole rectangular guide system.

In order to avoid so far as possible the condensation of pump fluid on the water-cooled walls of the vacuum envelope and the corrugated waveguide the cylindrical section of envelope R in the neighbourhood of the pump baffle is cooled by water at least 5 °C colder than the main water supply. A standard milk cooler comprising a refrigerator unit, a well lagged 40 gallon (180 litre)

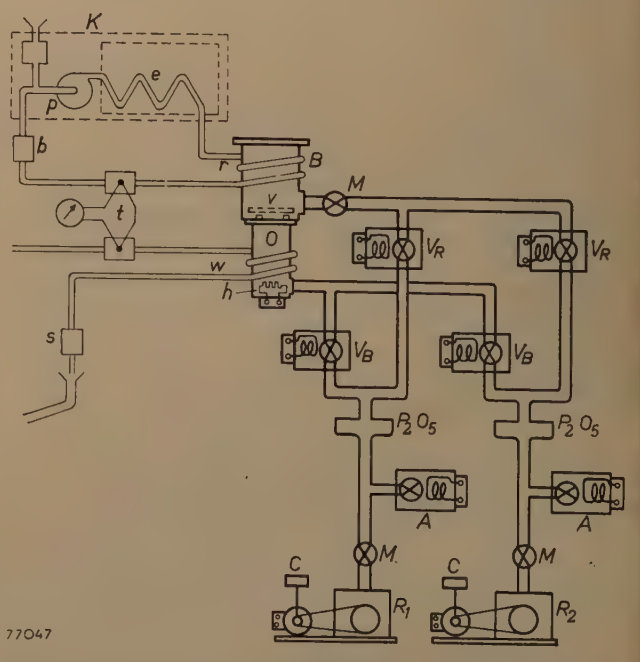

Fig. 14. Layout of the pumping system. O = oil diffusion pump with heater h, water cooling w and water flow switch s. R_1, R_2 = rotary pumps for backing and roughing. V_B = backing valves, V_R = roughing valves, A = air inlet valves. All these valves are magnetically operated. M = manual valves. C = centrifugal safety switches. P_2O_5 = moisture traps. B = baffle, with main valve v and refrigerated coils r; the water in this circuit is kept at least 5° C below that in the main cooling circuit by means of the refrigerator K with circulating pump p, heat exchanger e, water flow switch b (interlocked to the diffusion pump heater) and thermocouple t for monitoring temperature difference.

storage tank and a circulating pump, was adapted for this purpose. An electronic temperature controller was fitted which maintains the temperature of the water fed to the pump baffle at 5° C; this temperature is adequate in the Harwell installation, in which the main cooling water is recirculated and whose temperature never falls below 10 °C.

The layout of the pumping system is shown diagrammatically in *fig. 14* and the control panel and some of the component parts are seen in *fig. 15*.

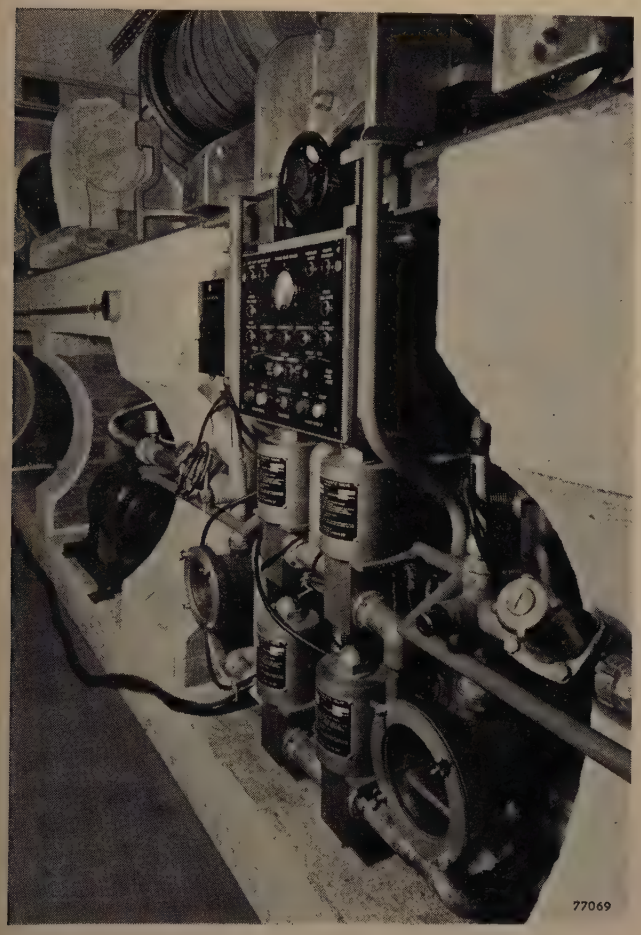

Fig. 15. Control panel and some of the component parts of the vacuum system. The four cylindrical containers under the panel are the magnetically operated valves. One of the rotary backing pumps is seen in the adjacent arch of the concrete table.

Two rotary vacuum pumps each with a displacement of 450 l/min are provided. While one of these is sufficient to maintain an adequate backing pressure for the diffusion pump, the second pump is useful when carrying out routine maintenance and also to save time when evacuating the whole system from atmospheric pressure (roughing).

The two pumps can be used either for backing or for roughing simultaneously, or each can carry out either function. In order to avoid the danger of mistakes in the control of these functions manual vacuum taps are not used; each pump is operated by means of a selector switch which controls a pair of magnetically operated valves.

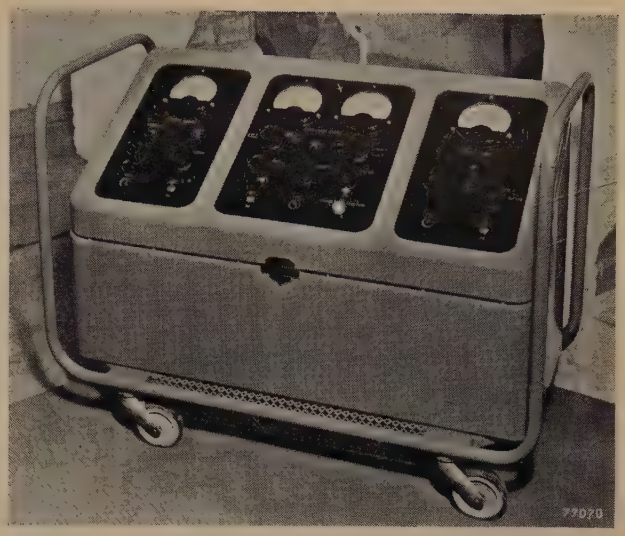

Fig. 16. Trolley housing the control units for all vacuum gauges (Pirani, Philips and triode ionization gauge).

Pirani, Philips and triode ionization gauges [13]) are provided for the measurement of rough, medium and fine vacuum respectively. The control units for all gauges are housed in the vacuum gauge trolley shown in *fig. 16*. The trolley is castor mounted and is connected to the gauge heads through a long flexible cable so that it may be moved around to facilitate leak hunting.

A number of protective devices connected with the vacuum system will be dealt with in a later section.

Modulator

The modulator which feeds the voltage pulses of 40-50 kV and 2 μsec duration to the magnetron and to the electron gun is shown in *fig. 17*. *Fig. 18* is a simplified circuit diagram.

The output of the main transformer *Tr* which is fed from a variable transformer Tr_1 is rectified and provides D.C. at 10-12 kV level. After smoothing, the output is fed through a ringing choke *L* and a gas triode Th_1 to the pulse forming network *D* ("delay line"). Owing to the inductance of the choke the pulse forming network will be charged to double the D.C. voltage supplied. When the ignitron *I* is triggered, the pulse forming network discharges through the ignitron and the primary of the 1:5 step-up pulse transformer P_1.

[13]) The ionization gauge control circuit is interesting in that a simple saturable reactor is used to stabilize the emission current at a preset value, in which case the plate current is a direct measure of the pressure in the system (Brit. Pat. Application 5377 of 1952).

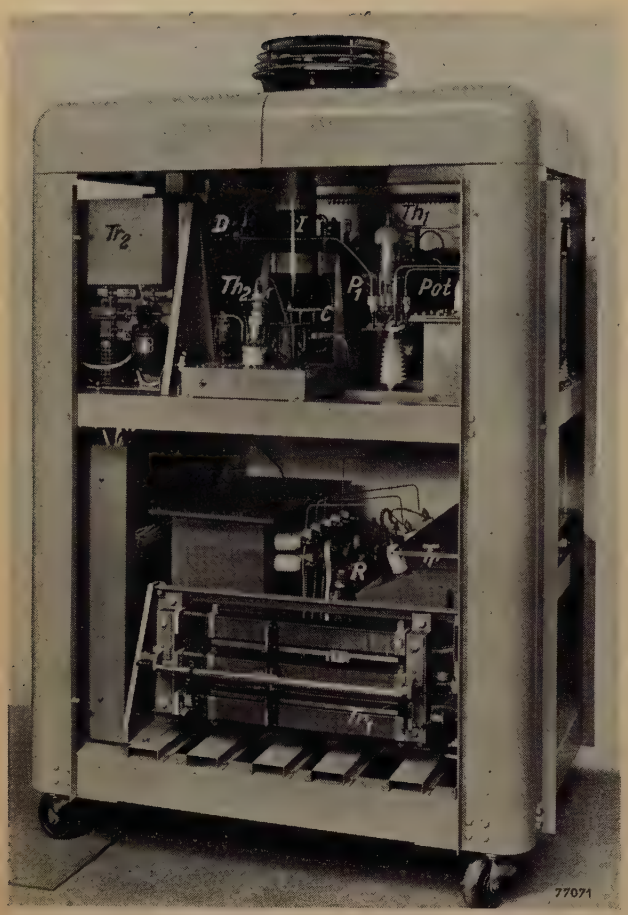

The rectangular pulse across the secondary of this transformer is fed to the magnetron cathode. For maximum energy transfer the impedance of the primary of P_1 is matched to that of the pulse forming network so that the voltage is divided equally between these two and a pulse voltage of about 10 kV is obtained on the primary and 40-50 kV on the secondary. The pulse transformer is bifilar wound so that the heater transformer for the magnetron can be at earth potential.

If the modulator were to operate at a fixed pulse repetition frequency the introduction of the series triode Th_1 would not be necessary since the time constant of the ringing choke L could then be adjusted so that the pulse forming network is charged to the maximum voltage just at the time of the occurrence of the next pulse. However, in practice the accelerator is used at a number of pulse repetition frequencies between 100 and 500 pulses per sec and the introduction of a cut-off valve is therefore essential. Furthermore the use of a suitable time constant in the grid circuit of Th_1 ensures that the pulse forming network does not start to charge

Fig. 17. Main modulator producing the voltage pulses of 40-50 kV and 2 μsec duration fed to the magnetron and to the electron gun, with covers removed. The letters correspond to those used in fig. 18.

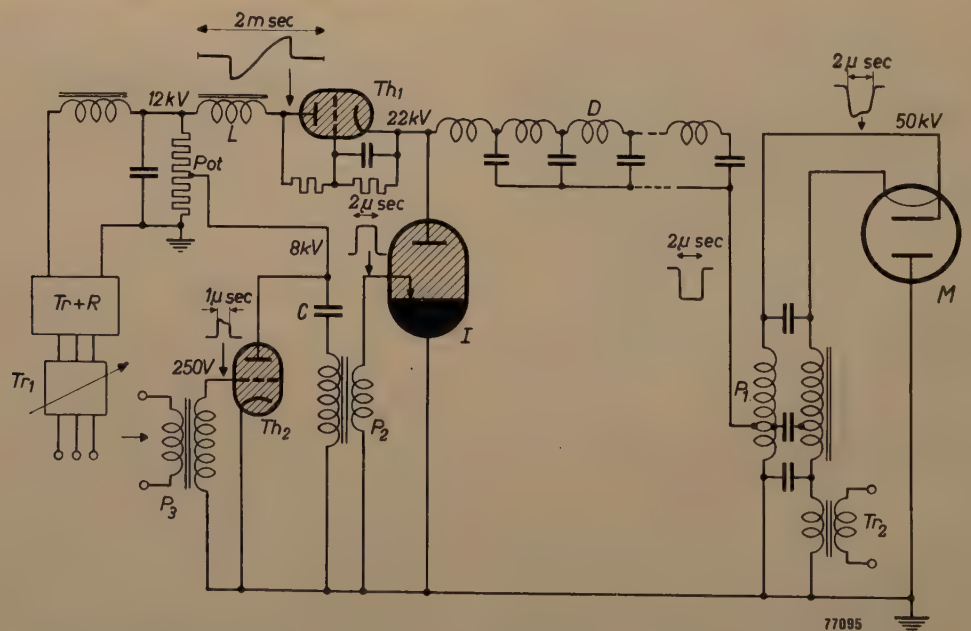

Fig. 18. Simplified circuit diagram of modulator, with waveforms obtained at several points. The pulse forming network D is periodically charged up from a 12 kV D.C. source via a ringing choke L and a cut-off gas valve Th_1. By discharging the network D through the ignitron I and the primary of step-up pulse transformer P_1, a rectangular voltage pulse is obtained on the magnetron M. The maximum pulse repetition frequency is 500 per second. The repetition frequency is controlled by triggering pulses fed through pulse transformer P_3 to the grid of the hydrogen thyratron Th_2 which on firing will discharge the capacitor C through the step-down pulse transformer P_2 thus delivering a high energy triggering pulse (2 kV, 300 A) to the igniter of the ignitron. $Tr + R$ = main transformer and rectifier. Tr_1 = variable transformer. Tr_2 = magnetron filament supply transformer.

until the ignitron discharge valve is completely de-ionized.

The choice of an ignitron as the discharge valve is rather unfortunate since it is inherently in its design prone to jitter and since its de-ionization time is relatively long. However, at the time the design was carried out, no hydrogen thyratron capable of handling 5 MW in the pulse was available. (A hydrogen thyratron to this specification is now made in the United States [14]).)

In order to reduce jitter two measures have been adopted. The first aims at assisting ionization by maintaining the ignitron bulb at as high a temperature as possible subject to not excessively increasing the de-ionization time of the ignitron. Experiments with a number of samples showed that a reasonable compromise temperature is 18 °C. The cooling water which is fed to the ignitron is therefore warmed to 18 °C by a 500 W immersion heater stabilized by an electronic temperature controller (Mullard type E 7594).

The second measure involves the use of a large triggering signal on the igniter of the ignitron. The signal is a pulse of 2 kV, 300 A obtained by the discharge of the 0.01 μF capacitor C through the step-down pulse transformer P_2 and the hydrogen thyratron Th_2. The capacitor C is charged to 8 kV from a potential divider (*Pot*) connected to the main high voltage line. The hydrogen thyratron Th_2 receives its triggering pulses from a blocking oscillator which thus controls the pulse repetition frequency of the modulator. The large triggering pulse of 600 kW peak power on the igniter of the ignitron reduces the maximum jitter to a value in the region of 0.1 μsec and the mean value is considerably less. On the other hand there is some evidence that the use of such a large triggering signal reduces somewhat the ignitron life and it becomes progressively more difficult to fire.

As a time somewhat longer than 1/10 μsec is necessary for oscillation to build up in the magnetron and the effective impedance during this period is very high (the current drawn is very small) the steep voltage rise on discharging the pulse forming network tends to produce a voltage spike on the magnetron in the early part of the pulse. The corresponding current spike would tend to produce unwanted modes of oscillation in the magnetron which generally cause sparking. The effect has been removed by the use of a choke in series and a series connected resistor and capacitor in parallel with the magnetron.

[14]) Electronics **26**, Febr. 1953, p. 158.

Rectangular waveguide system

The whole waveguide run from the dividing Tee is seen in fig. 6. As the system is evacuated right up to the magnetron, all the sections, bends and waveguide components (feedback bridges, phase shifters etc.) are connected together using standard vacuum type choke couplings. The feedback bridges, phase shifters and monitoring thermocouples will be described in some detail below. Each part of the waveguide which contains a discontinuity has been individually matched with irises to avoid reflections as far as possible: the voltage standing wave ratio (cf. note [6])) is not less than 0.98 for any individual part except for the phase shifters which cannot be matched to give this V.S.W.R. over their whole range of phase adjustment. The overall V.S.W.R. of the system (as measured above the dividing Tee, at low power and with the system at atmospheric pressure) varies between 0.8 and 0.97, depending on the position of the phase shifters.

Feedback bridges

The feedback bridges are of the type known as circular magic-Tee [15]) which is illustrated in *fig. 19a* (see also figs. 1, 5 and 6). It consists of two circular

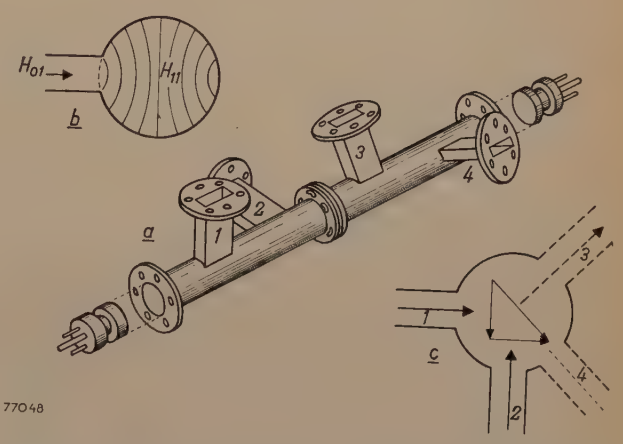

Fig. 19. *a*) Circular magic-Tee. It consists of two sections of circular waveguide, each section carrying two rectangular waveguide arms mutually at right angles and spaced axially by one wavelength. The two sections are joined by a rotatable vacuum joint and closed by an adjustable plunger for matching. *b*) Electric field lines of H_{11}-wave in the circular guide excited by H_{01}-wave in a rectangular waveguide arm. *c*) The two H_{11}-waves, excited in the circular waveguide by the rectangular waveguide arms *1* and *2*, have a resultant polarization at 45° (provided the phases are suitably adjusted). The sum of the two incident powers can then be drawn from rectangular waveguide arm *3*, and in the steady state no power will enter arm *4*.

[15]) The use of a circular magic-Tee in an accelerator feedback system was suggested by L. B. Mullett, see: L. B. Mullett and B. G. Loach, A. E. R. E. Report EL-R 93. See also: B. E. Kingdon, A circular waveguide magic-Tee and its application to high power microwave transmission, J. Brit. Inst. Rad. Engrs **13**, 275-287, 1953 (No. 5).

waveguides joined together at one end by a butt waveguide joint and a rotatable vacuum joint and closed at the other end by an adjustable non-contacting plunger and a vacuum end plate. To each section of circular guide are attached two rectangular waveguide arms, mutually at right angles and spaced axially by one wavelength in the circular guide. The principle of operation is as follows. Assume initially that equal powers are fed into two arms at right angles. Each will then give rise to an H_{11}-wave in the circular guide as shown in fig. 19*b*. (The radius of the circular guide is chosen so that a reasonably good impedance match is obtained as viewed from the rectangular guide.) The electric fields of both H_{11}-waves will be at right angles and of equal amplitude. Provided the phases are suitably adjusted the resultant polarization will be linear and at 45° to the individual polarizations. If one of the rectangular arms of the other circular section is now adjusted to be at 45° to the first two arms the sum of the two incident powers can be drawn from it; see fig. 19*c*.

When the ratio n of the two incident powers is not unity, the situation is similar but the angle between the resultant polarization and one input arm will now be $\varphi \neq 45°$. This angle is given by $\tan^2 \varphi = n$. By means of the rotatable vacuum joint the output arm from which the power is to be drawn can again be adjusted so that its axis is perpendicular to the resultant polarization. In the 15 MeV accelerator the practical value of n, i.e. the ratio of the power returned to the bridge from the guide to that supplied to the bridge by the magnetron, is $n = 1.28$. The angle φ in that case is about 46.5°. (This value of n will of course be correct only for one value of beam loading; cf. footnote [5]).

It might appear that under these ideal conditions the fourth arm, of the second circular guide section, serves no useful purpose. During the steady state of the pulse, when the power flow through the corrugated guide has reached its final value, no power will in fact enter this arm. However, during the first few tenths of a microsecond the power fed back will be less than the steady state value, and some power will enter the fourth arm. This power is dissipated in a matched load. (A similar situation will obtain even in the steady state when the beam current in the accelerator differs from its design value, but the power loss is small.)

It is convenient to use a matched water load [16]) in the fourth arm since it allows the power dissipated there to be measured during the setting up tests. This load is illustrated in *fig. 20* and some details are explained in the legend.

Comparing the circular magic-Tee with another type of feedback bridge, the rat-race, the former has the important advantage that it can be simply adapted to power addition ratios other than unity without upsetting the impedance match to the rectangular waveguide, viz, by changing the angle between the two sets of arms. On the other hand the rat-race is smaller and all arms are in the same plane, thereby eliminating the "staggered" sections of waveguide required for the circular magic-Tee. Incidentally it may be mentioned that in theory the two arms of each circular guide section could be in the same plane, but experimentally it is found that an appreciable amount of power fed into one arm then enters the arm perpendicular to it.

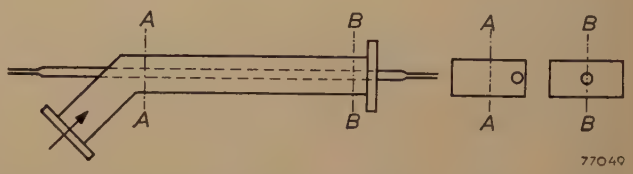

Fig. 20. Matched water load connected to fourth arm of each circular magic-Tee. A glass tube, through which the water flows, enters through a Wilson vacuum seal at one corner (see section *AA*) of a rectangular waveguide with a 45° bend and emerges centrally through a similar seal at the other end which is closed (section *BB*). Since the electric field near *AA* will be small, the discontinuity caused by the glass tube will not be important and little reflection of power will occur.

Phase shifters

The phase shifters used in this equipment consist essentially of a ceramic wedge placed in the rectangular waveguide parallel to its narrow face. The wedge is carried by two shafts and can be displaced perpendicular to the narrow face of the guide. The wedge will cause a delay in the propagation of the wave resulting in a phase change which depends on the position of the wedge and which attains its maximum value when the wedge occupies the centre of the broad face.

The displacement of the ceramic wedge involves the movement of a component inside the evacuated rectangular guide. Further, this movement must be effected by remote control as the phase shifters in the feedback loops may need to be adjusted during full power operation of the accelerator.

A magnetic coupling was developed for moving the phase shifters, which eliminates a vacuum seal on any moving member and therefore requires only a very small torque and the very minimum of maintenance. The coupling makes use of a horseshoe magnet which is supported on a bearing outside the vacuum system and which may be rotated about its axis by remote control. Magnetically coupled to

[16]) Brit. Pat. Application 24823 of 1952.

the magnet but inside a bell-housing attached to the guide and which forms part of the vacuum system is a soft iron pole piece mounted on a threaded shaft which actuates the ceramic wedge carriage. The shafts which carry the ceramic wedge are of silver steel and are separated by an odd multiple of the mean quarter wavelength in the guide in order to minimize mismatch.

Moving parts inside the vacuum are lubricated occasionally when convenient with "Apiezon" pump fluid. A unit of this type incorporated in the 3.5 MeV accelerator has been in operation for three years; it required servicing after about 18 months.

The position of the wedge in the waveguide is indicated remotely on a voltmeter by means of a potentiometer coupled through a gear box to the external rotating shaft. Limit switches are provided in the external driving mechanism to prevent the wedge jamming against the guide wall.

Monitoring thermocouples

The thermocouples used for power monitoring are of the usual waveguide type. Each thermocouple consists of a small pick-up loop in an evacuated bulb. The current induced in the loop by the wave in the guide heats the thermocouple junction, one end of which is connected to a copper foil flange, the other end being brought to an insulated top cap. The thermocouples are used in pairs, spaced by $^3/_4$ of a guide wavelength to reduce errors due to standing waves. The two thermocouples of one pair are connected in series and the polarities are arranged so that the output is taken from the two top caps.

The thermocouple mount is designed to provide a good vacuum seal on the rectangular waveguide and at the same time to allow the replacement of burnt-out thermocouples without an elaborate re-calibration procedure. The mount is shown in *fig. 21*. It will be seen that each thermocouple with its copper foil flange is clamped between a pair of annular discs; this assembly rests in a circular hole in a plate hard soldered to the waveguide and is sealed in position by a collar bolted on to the plate. For calibration a thermocouple pair is mounted in a separate waveguide section where the power flux can be measured directly using a water load. By rotating the disc assemblies the sensitivity of each thermocouple is adjusted so that the correct power values are indicated on the meter. The line of the axis of the guide is marked on the upper disc of each assembly and the thermocouples are transferred in this position to their proper place in the rectangular waveguide system. Using this method the calibration will be accurate to $\pm 5\%$ which is sufficient for the purpose.

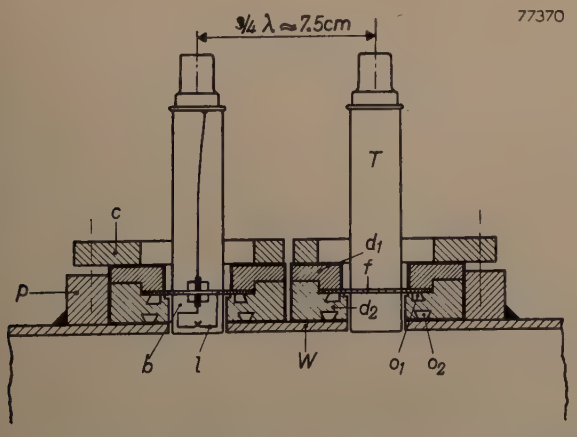

Fig. 21. Waveguide thermocouple mount. The thermocouples T are used in pairs, each being mounted in a rotatable disc assembly so that the sensitivity may be easily adjusted. l = pick-up loop. b = bulb. f = copper foil flange. d_1 and d_2 = discs. o_1 and o_2 = O-ring vacuum seals. p = plate soldered to waveguide wall W. c = collar for clamping the disc assembly in position.

Protective system

With a view to avoiding damage or loss of time in case of failure of any component or supply, a number of safety circuits have been provided. The description of the safety system will be restricted to indicating which components require protection in the event of a given failure, and the general type of indicators and circuits used.

A series of safety measures have been provided for the vacuum system. In the event of mains failure to the diffusion pump the two magnetically operated backing valves are closed so that the vacuum in the envelope is maintained, avoiding waste of time and preventing damage to the hot diffusion pump fluid. If the rotary backing pump ceases to function, due to failure of the mains supply to the pump, of the driving belt or of the motor, a centrifugal switch mechanically connected to the pump shaft switches off the diffusion pump and closes the backing valve; moreover this switch opens magnetically operated air inlet valves situated in the line to each of the two backing pumps, as a protection against oil from these pumps being sucked into the vacuum lines. Of course, the air inlet valve must not open until the backing valves have closed; this is ensured by increasing the time constant of the solenoid of the inlet valve by a large capacitor.

The same series of events will take place in the case of a general mains failure. No other automatic action is necessary in such an event since self-holding contactors are used in the switches so that

power is not re-applied automatically when the supply returns.

A rise of pressure in the vacuum system might also occur due to a vacuum leak while all components in the vacuum system are functioning normally. Such a rise of pressure, apart from cracking the pump fluid, would cause irreparable damage to the ionization gauge filament and the gun filament. Moreover, it would cause sparking in the rectangular waveguide or the corrugated guide and the resultant considerable mismatch would in turn produce severe sparking in the magnetron. To avoid these consequences the Philips gauge mentioned earlier incorporates an electronic relay system which operates if the pressure in the vacuum envelope rises above 10^{-3} mm Hg: this initiates the closing of all vacuum valves and at the same time switches off the modulator, gun filament supply, diffusion pump heater and all vacuum gauges.

The failure of cooling water supplies could cause even more costly damage to the magnetron, to the corrugated guide (due to differential expansion between it and the vacuum envelope), to the electron gun and to the diffusion pump. The water circuits therefore contain bucket-type switches, which in the event of water supply failure interrupt the mains supply.

Lastly, overloads in the three phase supply to the modulator, in the drive circuit, the main high tension circuit and the single phase supply to the focusing coils are monitored by relays. These relays in the D.C. circuits are actuated by the voltage drop across resistors and in the A.C. circuits by current transformers.

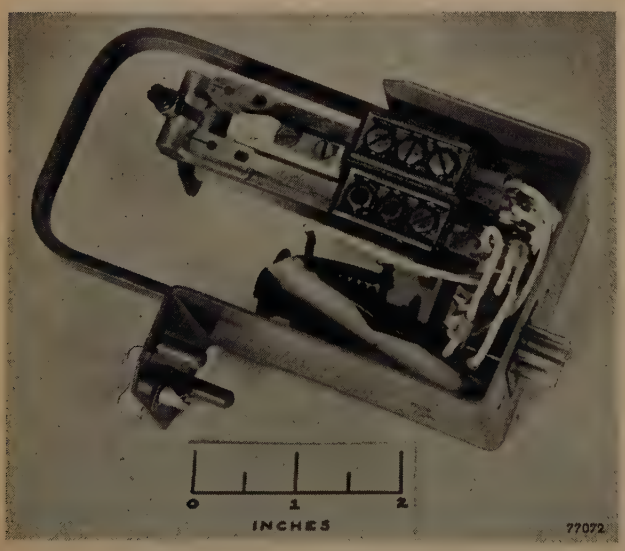

Fig. 22. Relay pack used in the protective circuits. If a relay failure occurs, the pack is unplugged and may be replaced by another one of the same type.

It has been stated that the protective system besides safeguarding the equipment from damage should minimize the loss of time due to failure of components. In any protective system of this extent

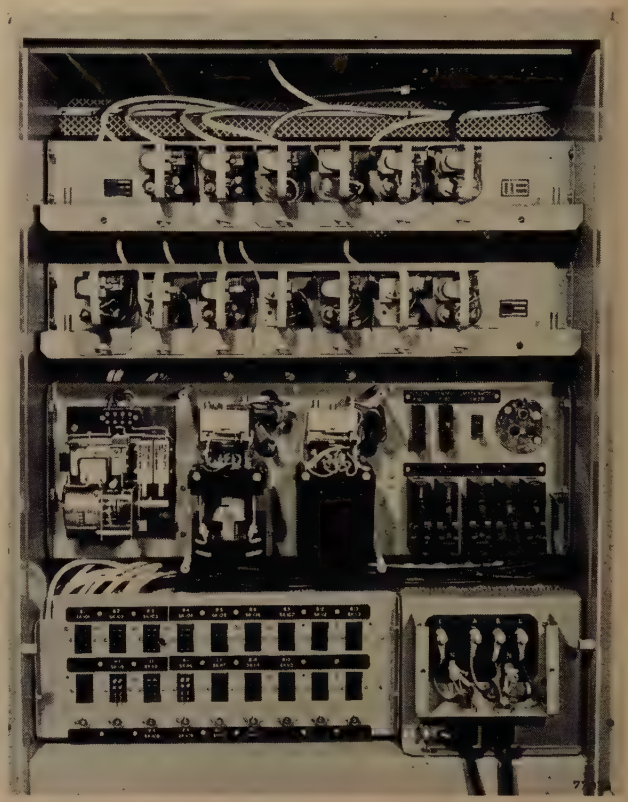

Fig. 23. View of the safety circuit panel of the modulator. Note the set of relay packs in the upper portion.

and intricacy, however, the factor of time loss due to failures in the protective system itself becomes important! The elements most liable to cause trouble are the relays with which most of the protective circuits are associated. Therefore a plug-in relay pack (*fig. 22*) has been developed which incorporates a standard Post Office type relay and which with very minor circuit modifications is used in all these circuits (*fig. 23*). Failure of any relay during service instead of necessitating a lengthy removal and replacement delay, merely requires the unplugging of the faulty pack and replacement by another of the same type. A coding system is used so that it is impossible to plug in a pack of the wrong type.

Control

As the accelerator shelter is not accessible while the apparatus is running, all adjustments required during operation must be made by remote control. In view of its position it is convenient to be able

to control the modulator remotely also[17]). The control desk (*fig. 24*) has been designed to carry out this dual purpose. It consists of seven easily removable panel units:

1) Main control panel. This includes push buttons for switching on valve heaters and anode supplies and for switching on and varying the high voltage output from the modulator. Meters are provided to monitor the voltage and current from the main rectifier circuit in the modulator. Also attached to this panel is the oscillator which generates the voltage pulses for controlling the modulator. Pulse repetition frequencies of 100, 200, 350 and 500 pulses per second may be selected by means of a switch. Alternatively an external source of triggering pulses may be connected by means of the same switch.

2) Magnetron control panel. This provides facilities for control and measurement of filament current, magnetic field, radio frequency power and frequency.

3) Controls more directly concerned with the electron beam. Here facilities for control of the gun filament current, for the measurement of the total power in the electron beam and of the X-ray output and finally for the control of phase and measurement of radio frequency power in each of the feedback loops are found.

4) Oscilloscope unit. This has a time base of either 12 μsec, 120 μsec or 12 msec. It may be used to monitor pulse voltage and current waveforms in the modulator or, for example, the current pulse produced by the scintillation from a crystal under the action of the X-rays generated. It also includes a 60 dB pulse amplifier connected to the output of a high-Q cavity wavemeter for frequency monitoring; this method of frequency measurement is useful since it demonstrates frequency changes during the magnetron pulse or the presence of even a very small amount of unwanted modes in the magnetron oscillation.

5) Safety circuits panel. This indicates the state of the various safety circuits by a series of green lamps. A red lamp is associated with each of the four high power circuits which are protected against current overload as explained in the previous chapter. When the overload protection operates, the red lamp lights and after the fault has been noted and cancelled by means of a push button on the

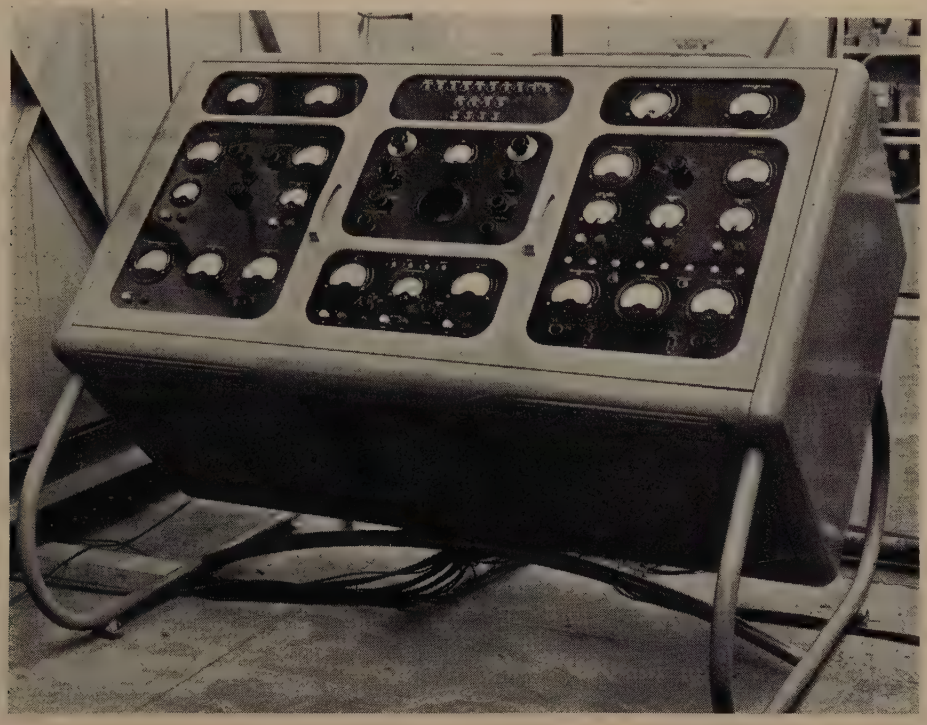

Fig. 24. Control desk of 15 MeV accelerator. It includes a main control panel (lowest centre), magnetron control panel (lower left hand), controls concerned with the electron beam (lower right hand), oscilloscope unit (middle centre), safety indicator panel (uppermost centre) and two subsidiary panels for checking the condition of the vacuum system and for various other meters.

[17]) In certain medical applications the modulator will be placed beside the accelerator, so that remote control is unavoidable.

same panel, the circuit can be switched on again.

6) and 7) Finally two small panels provide a remote indication of pressure from the ionization gauge circuit, of the temperature difference between the main and the refrigerated water supply and any other indications which may be required in a particular installation. At Harwell three hour-meters (not shown in fig. 24) indicating low tension circuits, high tension circuits and refrigerator compressor hours were installed in one of these small panels. The first two assist in compiling information on the valve life to be expected in various circuits.

C. TESTING AND PERFORMANCE

Measuring methods

The testing of the machine as a particle accelerator primarily involved the measurement of the electron energy and the beam power. No attempt was made to measure the beam current directly since this is more difficult and without very carefully designed measuring gear would yield no more than a very rough cross check on the value of current derived from the other two measurements.

Measurements of the X-ray intensity obtained and of the beam concentration (i.e. the radial distribution of the electrons in the beam) were also made. These characteristics will of course be of special importance when a similar machine is used for X-ray therapy.

The *total beam power* was measured by means of a constant flow water calorimeter. This consisted of a cylindrical brass container long enough to absorb all electrons and closed by a brass plug at one end and a thin copper foil at the other. The container was supported coaxially with the accelerator and with the copper foil facing the electron source so that the electrons tended to give up their energy in the water rather than in the walls of the container. The temperature rise of the water was monitored by a differential thermocouple. In these experiments the electrons emerged from the accelerator through a hole covered by a 0.002 inch (0.05 mm) beryllium copper foil. The loss of energy in this foil is very small but it causes considerable scattering. The calorimeter was therefore placed as close as possible to the foil to minimize the air gap and to prevent the loss of scattered electrons.

By adjusting the rate of flow of water so that the inlet and outlet temperatures differ by not more than 10 or 15 °C, and by arranging that these temperatures in so far as possible lie below and above ambient temperature, the heat loss to the air is made negligibly small.

The *electron energy* is determined, by the conventional method, from the radius of curvature of the electron path in a known magnetic field which is at right angles to the direction of motion. A schematic layout is shown in *fig. 25*. Two steel plates F_1 and F_2 with slits for the passage of the electrons are set up at right angles. Electrons from the accelerator pass through the slit S_1, traverse a 90° arc between the pole pieces of an electromagnet (required field intensity about 0.2 Wb/m²) and emerge through the slit S_2. After traversing a drift space 30 cm long they pass through a further slit S_3 to a collector. The current obtained from the collector is proportional to the number of electrons that leave the accelerator with an energy corresponding to the chosen value of the analyzing magnetic field.

The current pulse is amplified by a screened preamplifier close to the collector and then by a high-gain balanced amplifier; the output pulse is displayed on a high speed oscilloscope. In this way the duration of the electron pulse and the time distribution of electron energies occurring in the pulse may also be measured.

Since the electrons traverse a path of the order of 1 m length between the accelerator output window

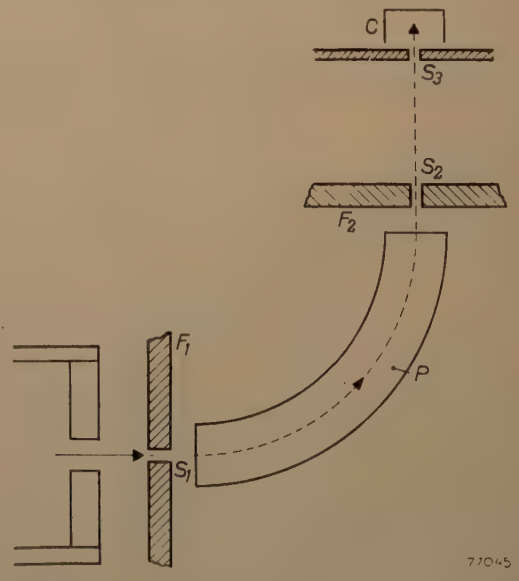

Fig. 25. Set-up for measuring the electron energy. The electrons emerging from the exit window of the accelerator pass through the slit S_1 and enter the magnetic field between the pole pieces P of an electromagnet. The field is adjusted so that the electrons describe a 90° arc and pass through the slit S_2 to collector C. (Of course, the magnetic field need be established only along the actual electron path, so that the pole pieces take the form of 90° arcs.)

and the collector, the scattering — if the path were at atmospheric pressure — would be considerable and the current pulse at the collector would be very small indeed. To avoid this the electrons pass through a similar beryllium copper foil window at S_1 and enter a tubular vacuum system which extends right up to the collector. The resultant scattering in the two foils and in the 1 inch path in air between the foils is not very serious since the pulse current is large and the absolute current value does not matter in these measurements.

Of course it would have been possible to avoid all scattering by joining the tubular vacuum system directly to the main vacuum system, which at the same time would eliminate the necessity of separate pumping. This scheme was not adopted, however, because of the physical difficulty of aligning accurately the considerable mass of the magnet and its associated trolley to the vacuum envelope. Moreover, it would have made it impossible to measure both the electron energy and beam power inside a short time interval (see below).

Another possible source of error has to be considered in the energy measurement. The mild steel plates F_1 and F_2 are used to eliminate the effects of the stray field of the analyzing magnet on the electron beam when it is near the target end of the corrugated waveguide. After passing through the slit S_1, however, an electron will be under the influence of the stray field of the magnet since the steel plates must be mounted some few inches away from the edges of the pole pieces to avoid affecting the uniformity of the analyzing magnetic field inside the pole gap. In order to allow for the slight deflection of the electrons in the stray field the magnetic field was measured along the path between S_1 and S_2 and the actual path of electrons entering and leaving with path normal to F_1 and F_2 was determined by numerical integration. The required correction can be expressed by an effective radius of curvature which is greater than the mean radius of the magnet poles.

The value of the mean *beam current* is derived from the measurements of the electron energy and the total beam power. The pulse current may then be calculated from the measured pulse duration. In order to obtain the correct current value it is necessary to ensure that conditions of operation do not change between the measurements of energy and beam power. The general procedure adopted therefore was to have as short a time delay as possible between these measurements. Since it requires quite some time to align the analyzing magnet to the system, the energy measurement was carried out first, followed as quickly as possible by the power measurement.

Measurements of the diameter of the electron beam emerging from the accelerator can be made by placing a piece of photographic paper in the beam. The paper quickly darkens under electron bombardment and gives a black central portion where the electron density is highest, surrounded by a gradually decreasing coloration. This method is quite useful for centering the beam and indicates that the electron density is high inside a diameter of 6 to 8 mm, but of course it gives only a qualitative

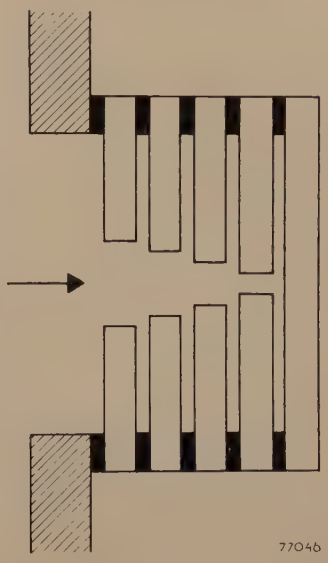

Fig. 26. Equipment for measuring the radial variation of electron current density in the beam. The beam strikes on a series of copper discs attached to the accelerator end plate, each thermally insulated from its neighbour and with an O-ring vacuum seal between adjacent discs. Progressively smaller holes are drilled in the discs, dividing the beam into a number of coaxial "tubes". The relative power in each "tube" is measured by means of a single turn cooling spiral.

estimate of the *radial electron distribution*. The system adopted to get a quantitative estimate is shown in *fig. 26*. To the end plate of the accelerator is attached a series of copper discs in which progressively smaller holes of $^3/_4$, $^3/_8$, $^1/_4$ and $^1/_8$ inch diameter are drilled. These discs divide the electron beam into a central core of $^1/_8''$ diameter and coaxial tubes with inner and outer diameters of $^1/_8$ and $^1/_4''$, $^1/_4$ and $^3/_8''$, and so on. A single turn cooling spiral is soldered to each disc and allows the relative powers in the various sections of the beam to be measured. The radial power distribution is also the radial current distribution, since there is no radial variation of electron energy.

Finally measurements of the *X-ray intensity* from a 4 mm platinum target were made using a concentric cylinder ionization chamber with 200 volts across a 1 mm gap [18]).

[18]) These measurements were made by Mr. G. S. Innes of St. Bartholomews Hospital, London.

Performance

The maximum energy obtained from the accelerator at low beam currents lay always between 14 and 15 MeV with a tendency towards the lower figure. The actual output achieved under any given conditions depends of course to a very marked extent on the frequency of operation, the magnetron power and the care with which the feedback loop phase shifters and the phase shifter between the two loops have been adjusted.

at the base and 1.1 μsec at the top giving a mean value of 1.3 μsec. The measured length of the current pulse through the magnetron was 1.85 μsec and the radio frequency power pulse will not be very much less. This appears to indicate that the time required to build up energy in the corrugated waveguide is of the order of 0.5 μsec.

The electrons emerging from the accelerator are not strictly mono-energetic but the spread of energy is reasonably small. The spread varies during

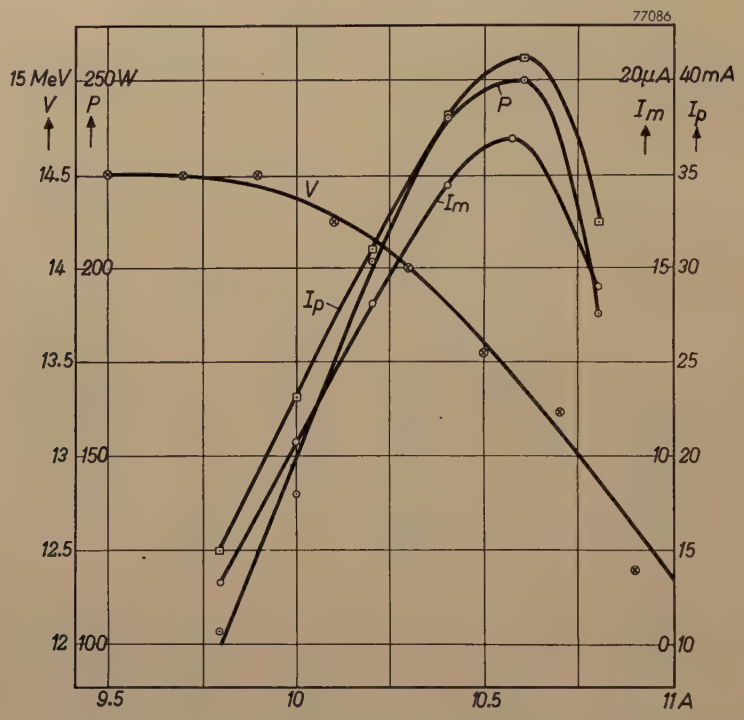

Fig. 27. Variation of electron energy V, beam power P and beam current (mean value I_m, pulse value I_p) with gun filament current (i.c. with beam loading) as measured in experiments with the 15 MeV linear accelerator. The magnetron pulse power was slightly more than 1.8 MW, frequency 2999 Mc/s, electron pulse duration 1.3 μsec, pulse repetition frequency 350 per sec. The measurements were obtained after reasonably careful adjustment of the phase shifters. It is seen that the actual performance falls somewhat short of the predicted values [19]) (15 MeV at 25 mA).

Fig. 27 shows graphically a typical set of measurements obtained after reasonably careful adjustments and with a magnetron which delivered slightly more than 1.8 MW in the pulse. It will be noted that with increasing gun filament current the beam power increases to a maximum and then falls off rapidly. This is due to the beam loading and consequent decrease of peak accelerating field which probably causes electrons to be slowed down to such an extent that they fall back behind the wave crest (region of peak accelerating field) and are lost.

The length of the electron pulse as measured on the oscilloscope display was found to be 1.5 μsec

the pulse and is approximately 7% (total width of spectrum) when the current has attained half its peak value. The spread is mainly accounted for by the occurrence of two quite distinct energy levels which are separated approximately 0.25 MeV in energy. Electrons of the lower energy level occur mainly in the first part of the pulse whereas electrons of the higher level are concentrated in the latter part. This is clearly demonstrated by *fig. 28* showing the appearance of the current pulse as the analyzing magnetic field is varied. The exact extent of the dip in the centre current pulse is difficult to determine owing to the finite resolving power of the analyzing system. The effect has also been noted by other workers in the field on other

[19]) Cf. also: C. W. Miller, Nature **171**, 297-298, 1953 (Febr. 14).

travelling wave accelerators. The authors are unable to advance any satisfactory explanation.

The radial variation of the current as measured by the series of copper discs and the calculated radial variation of current density are plotted in *fig. 29*. It will be seen that just under 60% of the current is contained inside a 5 mm radius and 50% inside a 4 mm radius.

The variation of X-ray intensity (dose rate) with gun filament current is shown in *fig. 30*. The beam current estimated from the power dissipated in the X-ray target is also given in this figure, to show the close correlation between current and X-ray

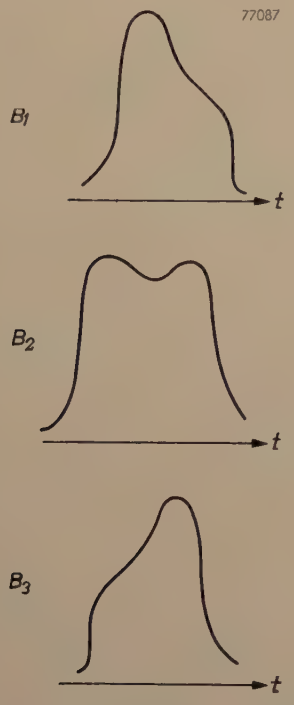

Fig. 28. Appearance of current pulse as obtained at the collector of the energy analyzer (fig. 25), for different values of the analyzing magnetic field ($B_3 > B_2 > B_1$). The oscillograms demonstrate the occurrence of two quite distinct energy levels, differing by about 0.25 MeV (as derived from the difference between B_3 and B_1).

intensity; the values of the current should not be taken as absolute values since there is considerably more heat loss associated with this measurement than with the water calorimeter. The efficiency of X-ray production in the heavy metal target will also be considerably greater than in the water target, i.e. more of the electron beam power will be in the X-rays emitted. In fact the current values appear to be about 20% low.

It will be seen from the graph that the radiation intensity peaks just before the current. This is as would be expected since the radiation intensity is proportional to the current and proportional to approximately the 2.7th power of the electron

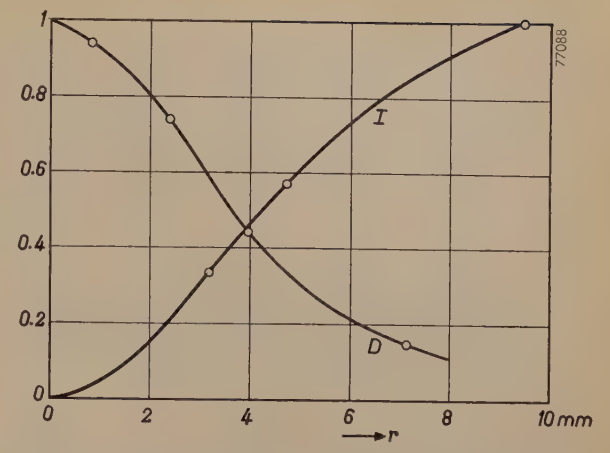

Fig. 29. Radial distribution of electrons in the beam. Curve *I*: relative current inside radius *r*. Curve *D*: relative current density at radius *r*.

energy. The energy is falling quite rapidly in the region of the beam current maximum.

All the measurements described above were made at a repetition frequency of 350 pulses per second. At Harwell the normal operating frequency is 400 pulses per second and in view of the danger of damage to the glass window of the magnetron, this must be considered a maximum for running periods in excess of 30 minutes or so. For short periods the magnetron may be operated (in this accelerator) at 500 pulses per second, when the maximum X-ray intensity is in the region of 2250 röntgen/minute at 1 metre from the target.

Acknowledgements

The thanks of the authors are due to the Director of the Atomic Energy Research Establishment and

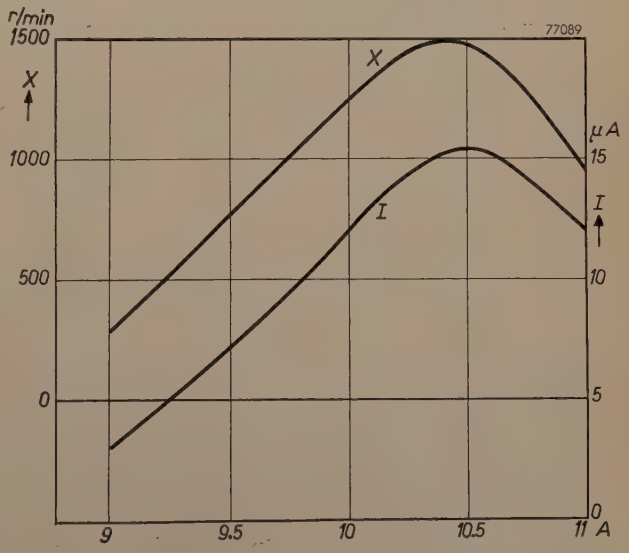

Fig. 30. Variation of the X-ray output (in röntgen/min at 1 m distance from a 4 mm platinum target) with gun filament current (curve *X*). The curve *I* represents the variation of beam current estimated from the power dissipated in the target cooling water.

to the Directors of the Mullard Radio Valve Company for permission to publish this article.

The authors also wish to thank friends at A.E.R.E. for their valuable cooperation, especially E.R. Wiblin and B. L. Tozer who assisted greatly during the construction and installation of the accelerator, and lastly their colleagues at Mullard Research Laboratories without whose untiring efforts this project could not have been completed in two years.

Summary of parts A, B, C. The linear electron accelerator described in this article was destined for nuclear physics work at the Atomic Energy Research Establishment, Harwell. Its design was based on a performance of 15 MeV electron energy and 25 mA beam pulse current, with a corrugated waveguide of length about 6 metres, and using a magnetron operating at 3000 Mc/s with 1.8 MW pulse output. The electron energy to be expected in a system with feedback was computed for different values of the guide parameter a/λ, using a formula which takes into account the heavy beam loading. As a result it was decided to divide the waveguide into two sections each of 3 metre length, each with its own feedback loop, and to use a value $a/\lambda = 0.168$, the electrons travelling at a stable phase 35° in front of the wave crest. In this way, since it is possible to adjust the phase between wave and electron after the first waveguide section, the frequency sensitivity of the accelerator is reduced to a workable value, having regard to the magnetron stability and practical machining tolerances.

To ensure easy assembly, dismantling and re-assembly without re-adjustment, the corrugated waveguide with its associated parts is mounted on six three-wheeled trolleys running on rails. The trolleys if necessary can be supported from above, thereby facilitating a conversion of the design to a machine for medical use. After a brief survey of the characteristics of the main components of the complete installation, a number of components are described more fully. This description includes the corrugated waveguide which consists of 316 cells, and whose machining and watercooling are discussed; — the electron gun with vacuum valve, and with gun filament supply stabilized by means of a "magnetic diode" circuit; — the focusing coil system surrounding the guide and divided into six sections, fed from six independent power supply units whose stabilized output current may be adjusted to give maximum electron beam current; — the vacuum system, consisting of a diffusion pump of 1500 litres/sec unbaffled pumping speed, two rotary backing (or roughing) pumps controlled by magnetically operated valves, and an extensive gauging and protective system; — the radar type modulator placed on top of the concrete shelter in which the accelerator is housed and feeding 40-50 kV pulses of 2 μsec duration with a maximum jitter of 0.1 μsec to the magnetron and to the electron gun; — the rectangular waveguide system evacuated to a low pressure to prevent sparking and incorporating the two feedback bridges (circular magic-Tee's, that are easily adaptable to the power addition ratios other than unity required in this system), the phase shifters which are adjusted by remote control using a specially developed magnetic coupling in order to avoid vacuum seals on moving members, and the power monitoring waveguide thermocouples required for adjusting the phase to give maximum power flux; — finally the general lay-out, the details of the protective system and the control and measuring equipment on the control desk.

The last part contains a description of the methods used for measuring the electron energy, the beam power (the beam current being derived from these two), the energy spectrum, the X-ray output and the radial variation of electron density in the beam. The energy obtained with an electron beam current of 25 mA when the phases in the feedback loops are carefully adjusted is between 14 and 15 MeV. 50% of the beam power is concentrated on the target within a circle of 8 mm diameter. The maximum X-ray output measured at 1 m distance from the target is 2250 röntgen per minute.

A LARGE-SCREEN TELEVISION PROJECTOR

by J. HAANTJES and C. J. van LOON.

621.397.62:535.88

Television pictures suitable for presentation in cinemas have to be about 10× larger than those given by domestic receivers. The problems of producing such a large image have been surmounted, as will be seen from the following description of the large projector designed by Philips. Prototypes of this equipment have for some years been available for demonstration to visitors to the Philips Research Laboratory and the E.L.A. Studio (a studio for the recording and reproduction of sound and for film projection). The projector has now been in actual production for some time.

In some countries television has made great strides, notably in the United States where the number of receivers in use is estimated at 20 million; in Great Britain there are some 2 million sets in use. There is little doubt that rapid expansion will follow in other countries and that, there too, television is due to play a growing role in the field of entertainment.

There are no longer any technical reasons why the use of television should be restricted to private entertainment in the home. The fact that it is possible to produce images several yards in width offers considerable scope for the extension of television applications. One such application is in the cinema. In the United States many cinemas are now equipped for showing television pictures [1]), but further developments in this direction depend on non-technical factors; these will not be discussed here.

An entirely different use for television arises from events which take place in locations where the public cannot be admitted, but which large numbers of people should nevertheless have an opportunity of seeing. In such cases the television camera and a large projector can be employed in a "closed circuit". A typical example of this field of application is in college hospitals, where the medical students are thus enabled to see on the screen in the lecture room an operation being performed just as though they were standing beside the surgeon. In 1949 Philips had already demonstrated this method at the University at Leiden [2]).

The size of the picture in the ordinary domestic television receiver has increased considerably since 1948. In that year the screen of the largest tube then in use was 30 cm in diameter, but there was much demand for a larger screen. However, as in other spheres (the automobile industry for example), European techniques have not met the demand along the same lines as in the United States. There, the most popular screen diameter is 50 cm, the largest being 75 cm. In Europe the largest "direct vision" tube normally obtainable is 43 cm. For pictures larger than this, projection television is normally used. In this system only a small tube is used, the very bright image thus obtained being enlarged to a considerable size by optical means. As far back as 1948 Philips had brought this system to a high state of perfection [3]) and, for private viewing, both systems are now in use. It is not yet certain which of the two systems will become the more popular.

Television for large audiences is another matter; a picture several feet in width is then required and projection is the obvious solution; many difficulties had to be surmounted, however, before satisfactory results were obtained.

The "Mammoth" projector, designed by Philips for use in halls (type No. EL 5750) gives a picture 4 × 3 metres in size using a tube only slightly larger than the kind found in home projection sets, in conjunction with an optical system with wide aperture.

The main difficulty in this system is that of obtaining sufficient light; this question is therefore considered first.

The necessary luminous flux

In making an estimate of the luminous flux required from the cathode-ray tube to give satis-

[1]) According to a recent estimate this number has increased from 1 in 1949 to 75 in 1952, divided among 37 cities. See N. L. Halpern, Theater television progress, J. Soc. Mot. Pict. Telev. Engrs. **59**, 140-143, Aug. 1952.

[2]) Philips tech. Rev. **11**, 42, 1949-50.

[3]) See the series of articles: A Projection Television Receiver, Philips tech. Rev. **10**, 1948-49:
I. pp. 69-78, P. M. van Alphen and H. Rinia, The optical system for the projection.
II. pp. 97-104, J. de Gier, The cathode-ray tube.
III. pp. 125-134, G. J. Siezen and F. Kerkhof, The 25 kV anode voltage supply unit.
IV. pp. 307-317, J. Haantjes and F. Kerkhof, The circuits for deflecting the electron beam.
V. pp. 364-370, J. Haantjes and F. Kerkhof, The synchronisation.

factory results in a darkened hall we cannot do better than assume the operating conditions in cinemas. A film projector with shutter rotating, but without film, is considered to give satisfactory screen luminance [4]) when this is equal to 34 nit [4]). To ascertain the luminance when the film is being exhibited this value must be multiplied by the transmission factor of the film; at the most transparent parts this is seldom more [5]) than 0.5. A television image having a maximum luminance of 17 nit can in this respect be regarded as on a par with cinema pictures.

Let us denote the area of the projection screen in square metres by S. If the screen reflects wholly in accordance with Lambert's law, that is to say if it diffuses incident light in accordance with the cosine law within a solid angle of 2π, a luminous flux of $17\pi\ S$ would have to reach it to produce a luminance of 17 nt.

It is preferable to work with average instead of i.e. one which reflects more in the direction of the normal and less towards the wings than would be in accordance with Lambert's law. This process cannot be carried too far, however, as the solid angle within which observers see the image sufficiently brightly is then too small.

In our own experience optimum selectivity is that which produces a gain in luminance by a factor of 3 in the direction perpendicular to the screen and, with a screen of this kind, an incident luminous flux of $^1/_3 \times 0.3 \times 17\pi\ S \approx 5\ S$ lumens is sufficient.

This luminous flux represents only a part of the flux that has to be emitted by the cathode-ray tube, as some of it is lost in the optical system used for the projection. Even with a system having a very large aperture such as the Schmidt system, about which we shall speak presently, only some 30 % of the emitted light reaches the screen. Hence the cathode-ray tube must be capable of yielding $5\ S/0.3 \approx 17\ S$ lumens.

Fig. 1. Cathode-ray tube type MW 13-16 for large projection of television pictures. Screen dia. 12 cm. The H.T. terminal is seen on the lower right: the glass funnel and the ribbed cone of the tube serve to increase the creepage paths.

maximum values, as these are more easily measured. The average luminance can be assumed to be about 30% of the maximum, so that the average luminous flux would have to be $0.3 \times 17\ \pi\ S$.

Appreciably less is needed if use be made of a screen having a selective reflection characteristic,

[4]) The Commission Internationale de l'Eclairage recommends the use of the term "luminance" instead of brightness, and as units of luminance the nit and the stilb (abbrev. nt and sb): 1 nt = 10^4 sb = 1 candela (international candle) per m^2 = 1 lumen per m^2 per unit solid angle. The relationship between this and the much used units apostilb and footlambert is: 1 nt = π apostilb = 0.292 footlamberts. Hence 34 nt = 107 apostilb = 10 footlamberts.

[5]) A. Cazalas, Ann. Télécomm. 5, 298-306, 1950.

The projection tube

The cathode-ray tube with which the Mammoth projector is equipped is the MW 13-16 (*fig. 1*), of which the effective screen diameter is 12 cm, the working voltage being 50 kV. The beam current may reach a peak value of 2 mA, with an average of 0.5 mA; hence the rated average load on the fluorescent screen is a maximum of 25 W. Forced air-cooling is necessary to prevent the screen from cracking.

The fluorescent screen consists of silicates, all of which fluoresce in different colours but which, when mixed in certain proportions, emit white light

(colour temperature 6500 °K). A layer of aluminium is applied to the inside of the screen ("metal backing") to reflect the fluorescent light emitted rearwards, thus ensuring that this light is not lost [6]). With the metal backing the efficiency of the particular silicate mixture used is 2.5 candela/W, so that the MW 13-16 tube is capable of supplying a luminous flux of $2.5 \times 25 \times \pi \approx 200$ lm.

According to the estimate in the previous paragraph a screen area S is required to give $17S$ lumens, and this tube therefore emits enough light for a projection screen of area $S = 200/17 \approx 12$ m², i.e. 4×3 metres.

At the brighter parts of the image the beam current momentarily exceeds the average of 0.5 mA, and the tube is then working at a point where the fluorescence exhibits saturation with any increase in current [7]), i.e. the light yield is no longer proportional to the increase in current. At the peak value of the current (2 mA) the luminous flux is 600 lm.

The focusing of the electron beam must be very precise, as will be appreciated when it is remembered that the image on the screen of the tube is only 72×96 mm in size. Deflection of the beam is accompanied by a certain amount of defocusing: it is essential, however, that the light spot be quite clearly defined at the edges of the picture. Efforts can be made to compensate for deflection defocusing by making the focusing current vary in a certain manner with the deflection current (both focusing and deflection are electromagnetic), but it is considered preferable to eliminate the defect at its source as far as possible. Deflection defocusing is dependent on the three-dimensional distribution of the deflection fields; for this reason much thought has been given to the design of the deflection coils so that they will produce the best possible field distribution. Furthermore, deflection defocusing is reduced according as the electron beam is reduced in width at the points where the deflection fields operate. Hence the narrowest possible beam is employed.

In this way deflection defocusing has been reduced to a minimum and no compensation is necessary.

The optical system

The optical system must be capable of producing on the projection screen a highly magnified image of the picture on the tube; in the present case this represents a linear magnification of roughly $40\times$.

Special consideration must be given to the following points in the design of such a system.

1) The system must gather as much light as possible from the cathode-ray tube.
2) The quality of the image must be such that a television picture of 625 lines is not noticeably reduced in contrast or detail.
3) The dimensions of mirrors and correcting plates should be as small as possible, as the cost of these components rises very steeply with the size.

Reflecting system

A system which most nearly approaches these conditions is the Schmidt system, which has already been mentioned in numerous articles in this Review [8, 9]). It consists of a concave spherical mirror and an aspherical correcting plate mounted at the centre of curvature of the mirror (*fig. 2*). The main advantage of a mirror as compared with lenses as principal component is that mirrors are free from chromatic aberration and, in contrast with equivalent lens systems, exhibit less spherical aberration and are much less costly. Image defects such as coma and astigmatism are avoided by mounting a diaphragm at the centre of curvature [10]).

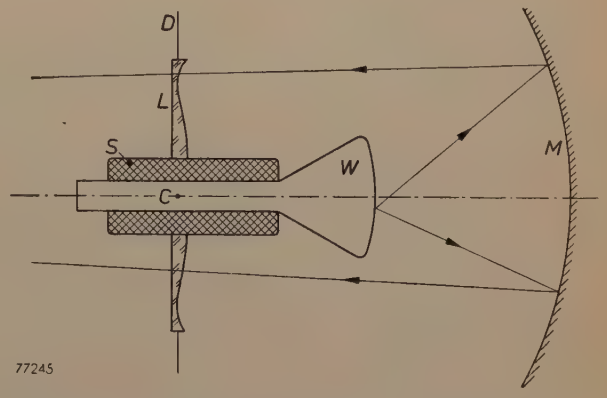

Fig. 2. Diagrammatic cross-section of the optical system. W cathode-ray tube with focusing and deflection coils S. M spherical mirror; L Schmidt correcting plate; D diaphragm; The planes of D and L pass through the centre of curvature C of the mirror.

The only defects of the third order then remaining are the spherical aberration and field curvature; the first is removed by using the correcting plate already

[6]) See article II, referred to in footnote [3]), in particular pp. 101-103.

[7]) A. Bril and F. A. Kröger, Philips tech. Rev. **12**, 120-128, 1950.

[8]) H. Rinia and P. M. van Alphen, Philips tech. Rev. **9**, 349-356, 1947-48.

[9]) See article I, referred to in footnote [3]).

[10]) See e.g. W. de Groot, Optical aberrations in lens and mirror systems, Philips tech. Rev. **9**, 301-308, 1947-48.

mentioned, and the second by curving the light-emitting surface, i.e. the screen of the cathode-ray tube, to a radius equal to the focal length of the system, and mounting it so as to be practically concentric with the mirror.

Optical systems made along these lines have a very wide aperture, they are relatively inexpensive to produce and, on plane surfaces, they give an image that is subject only to defects of the fifth and higher orders, and to an imperceptible chromatic aberration in the correcting plate.

Light-gathering power

We shall now determine the extent of the light-gathering power, that is, the ratio of the luminous flux entering the optical system to that emitted by the object, in this case the screen of the cathode-ray tube. For the moment we shall disregard losses of light due to absorption, imperfect reflection and masking effects: in other words we shall assume that the emitted luminous flux is equal to the incident flux.

To do this we make use of Abbe's law which states that when a luminous object is observed through a loss-free optical system, the luminance of the image as observed is equal to that of the object.

Let us denote the luminance of the image on the cathode-ray tube by L, the illumination on the projection screen by E, the diameter of the correcting plate by D and the distance from this plate to the projection screen by d. Then, in accordance with Abbe's law:

$$E = \frac{\frac{\pi}{4} D^2}{d^2} L.$$

The total luminous flux on the projection screen (area S_2) is therefore:

$$E S_2 = \frac{\frac{\pi}{4} D^2}{d^2} L S_2. \quad . \quad . \quad . \quad . \quad (1)$$

According to simple laws of geometrical optics the following relationship exists between d_1, the focal length f and the linear magnification M:

$$d = (M-1)f, \quad . \quad . \quad . \quad . \quad . \quad . \quad (2)$$

whilst

$$S_2 = M^2 S_1, \quad . \quad . \quad . \quad . \quad . \quad . \quad (3)$$

where S_1 is the area of the image on the cathode-ray tube. Substituting (2) and (3) in (1) ,we then have:

$$E S_2 = \frac{\pi}{4} \left(\frac{D}{f}\right)^2 \left(\frac{M}{M-1}\right)^2 L S_1,$$

for which, applied to the present case, where $M \gg 1$, we may write:

$$E S_2 = \frac{\pi}{4} \left(\frac{D}{f}\right)^2 L S_1. \quad . \quad . \quad . \quad . \quad (4)$$

It will be seen that, of the two parameters D and f which we have introduced in relation to the optical system, only their ratio, the so-called f-number D/f appears in equation (4). This equation states that, in order to obtain the optimum amount of light from the system, D/f must be as large as possible. At the same time the quality of the reproduction imposes a limit on D/f which experience shows to be roughly 1.4.

Another conclusion that may be drawn from (4) is that, since the luminous flux emitted by the cathode-ray tube is $\pi L S_1$, the fraction of this that reaches the optical system (i.e. the light-gathering power) will be $^1/_4(D/f)^2$. Taking D/f to be 1.4, this will be 0.5. (As explained in article I, referred to in footnote [3]), the light-gathering power is equal to the square of the numerical aperture, which in this case is 0.7.)

In practice the system is not free from losses; light is lost at the mirror, whose reflection coefficient is about 0.85; the cathode-ray tube itself intercepts some of the reflected light and the correcting plate reflects slightly. Consequently the luminous flux from the optical system is not more than 30% of the flux emitted by the cathode-ray tube, viz. the value which we have already employed in the preceding section.

Some of the light lost emerges from the system as scattered light, and this is a disadvantage as it reduces the contrasts in the image; light-scatter must therefore be avoided as much as possible, and this is done in the usual way by giving the interior of the optical system a dull black finish.

Dimensioning of the optical system

In order to ensure that the concave mirror will not limit the effective cone of light, the diameter of this mirror must be equal to at least $2f$. We have already seen that the diamter D of the correcting plate should be roughly $1.4f$.

The principal dimensions of the optical system are thus proportional to the focal length f. Hence to ensure compactness we shall want f to be as small as possible. On the other hand f cannot be made too small, as the image angle then becomes so large that the quality of the picture suffers, especially at the edges, where optical defects of the 5th and higher orders are mainly in evidence. In the Schmidt system the practical limit occurs at $f = 1.7$ times

the maximum dimensions of the object which, in our case, is the diameter of the fluorescent screen of the tube.

This diameter is itself subject to a lower limit. If the screen diameter — i.e. the size of the fluorescent image — is too small, one or more of the following difficulties is encountered:

1) Light saturation of the phosphor — even with the beam current below the maximum limit, the energy density on the light spot may be too high.
2) Heat dissipation — in a smaller area, simple air-cooling would not be adequate — the screen would deteriorate rapidly [11]) or even be in danger of cracking.
3) Size of light spot — to obtain a sufficiently small light spot, higher tube voltages would be necessary.

As a compromise between optical requirements and tube limitations a screen diameter of 12 cm was adopted.

To produce a picture diagonal of 5 m on the projection screen the magnification will be $M = 500/12 \approx 40\times$. From equation (2) it follows that the distance d from the optical system to the screen should then be about 8 m. Should the circumstances warrant a greater distance, the optical system would have to have a greater focal length. This would not affect the quality of the picture, but the equipment would have to be larger and more costly, without yielding the slightest gain in the luminance of the projected image, as will be seen from equation (4). (As will be shown presently, the design of the equipment is such that the need for a larger projection distance is unlikely to arise.)

The correcting plate

With a given correcting plate the Schmidt system gives good reproduction only when the magnification does not differ by more than 10% from the designed value. For greater variation of the enlargement different correcting plates are necessary. The Mammoth projector is supplied with a correcting plate adapted to the chosen projection distance; these plates are made from "Perspex" by turning them on a lathe.

Fig. 3 depicts the optical system in the projector,

[11]) A. Bril and H. A. Klasens, Intrinsic efficiencies of phosphors unter cathode-ray exitation, Philips Res. Rep. 7, 401-420, 1952 (No. 6).

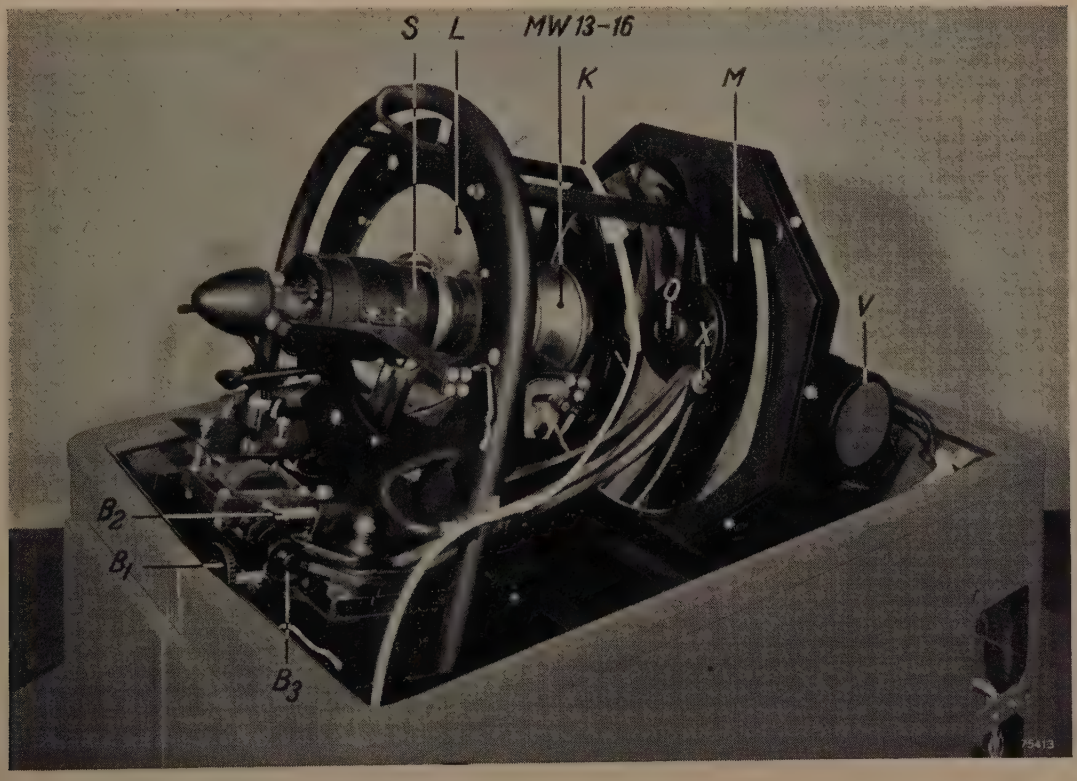

Fig. 3. The optical system in the Mammoth projector (with cover removed). S focusing and deflection coils on the cathode-ray tube MW 13-16. V motor driving blower at rear of the spherical mirror to blow cooling air through aperture O on to the screen of the tube. B_1 main adjustment for distance between tube screen and mirror. When a new tube is inserted, the axis of the tube must also be aligned with the principal axis of the mirror; hence the tube can be rotated on two axes, viz. with knob B_2 horizontally (X is one of the pivoting points) and with knob B_3 on a roughly vertical axis. K is the H.T. cable and L the correcting plate.

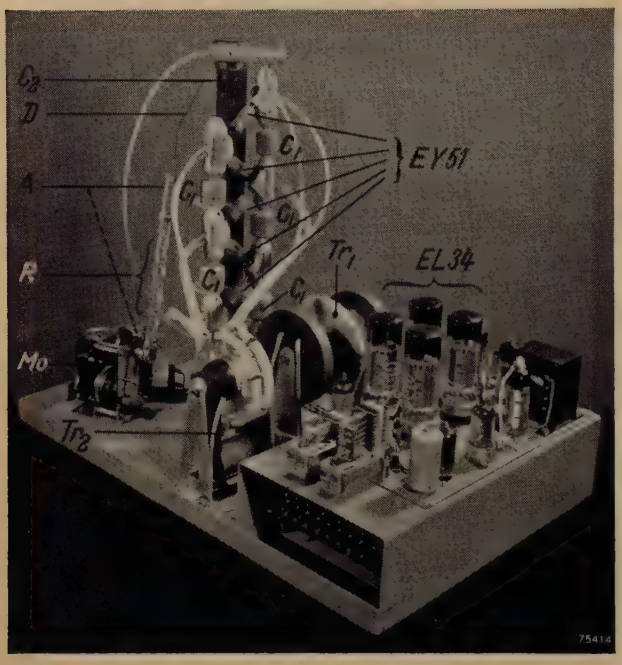

Fig. 4. Stabilized generator for 50 kV at an average current of 0.5 mA, as used in the Mammoth projector. In foreground: chassis with oscillator, control and protecting relay. The oscillator (frequency 20-25 kc/s) includes four valves type EL 34 and a transformer Tr_1. The oscillator voltage is rectified by six rectifier valves EY 51 with six capacitors C_1 in a cascade circuit (only 5 stages are visible in the photograph). A reservoir capacitor C_2 is included between the output terminals. Heater current for the rectifiers is obtained from a transformer Tr_2 which is fed from the oscillator. Tr_1 and Tr_2 both have Ferroxcube cores.

A is an insulated arm to which a series of resistors R and a contact wire D are attached. When the oscillator is switched off the arm assumes the position depicted, whereby D makes contact with the H.T. side of C_2. The capacitors are thus discharged across the resistors R, so as to eliminate all hazardous voltages. When the oscillator is switched on, a motor Mo moves this arm over to the position shown by the dotted line, and contact between D and C_2 is thus broken.

regarding which further details will be found in the subscript. Replacement of the cathode-ray tube necessitates only one or two simple operations, and adjusting knobs are provided for aligning the tube to its optimum position in relation to the mirror (the screen of the tube should be almost concentric with the spherical mirror, and the axis of the tube must coincide with the principal axis of the mirror). The whole operation of tube replacement and alignment takes only two minutes. The correcting plate is permanently mounted in the correct position with respect to the mirror.

The 50 kV D.C. supply

A number of methods of generating the high D.C. voltage needed for cathode-ray tubes have already been described in this Review [12]). In particular, mention was made of the generator designed for large television projection, and this generator is employed in the Mammoth projector. It consists of a valve oscillator operating at a frequency between 20 and 25 kc/s and delivering an A.C.voltage which is rectified to a high D.C. voltage by means of a circuit of rectifying valves and capacitors in cascade. The heaters of the rectifier valves are fed with high frequency current from the oscillator. A control system ensures a practically constant output voltage between no-load and full load, but with higher loads the voltage drops sharply, so that in the event of a short-circuit the current is very little more than on full load. In contrast to the method described in article [12]), the control potential in the present instance is in effect the difference between two D.C. voltages, one of which is proportional to the oscillator voltage, the other being a reference voltage maintained at a constant value by a stabilizer tube.

Should either the D.C. current or the voltage exceed a certain value owing to a defect in the control system, the generator is automatically switched off.

The H.T. generator of the projector consists of a single unit as depicted in *fig. 4*; further details are contained in the subscript.

Fig. 5. The Mammoth projector (Type EL 5750) mounted in front of the first row of seats in a hall. The projectionist takes his place behind the main body, between the "wings". The unit is so low that projectionist and public have an unobstructed view of the screen.

[12]) J. J. P. Valeton, Philips tech. Rev. **14**, 21-32, 1952.

Construction details

In the design of the Mammoth projector the ultimate aim was to ensure facility in operation and a compact, self-contained unit; this takes the form of a main central part, with two "wings" (*figs.* 5 and 6) between which the projectionist is stationed.

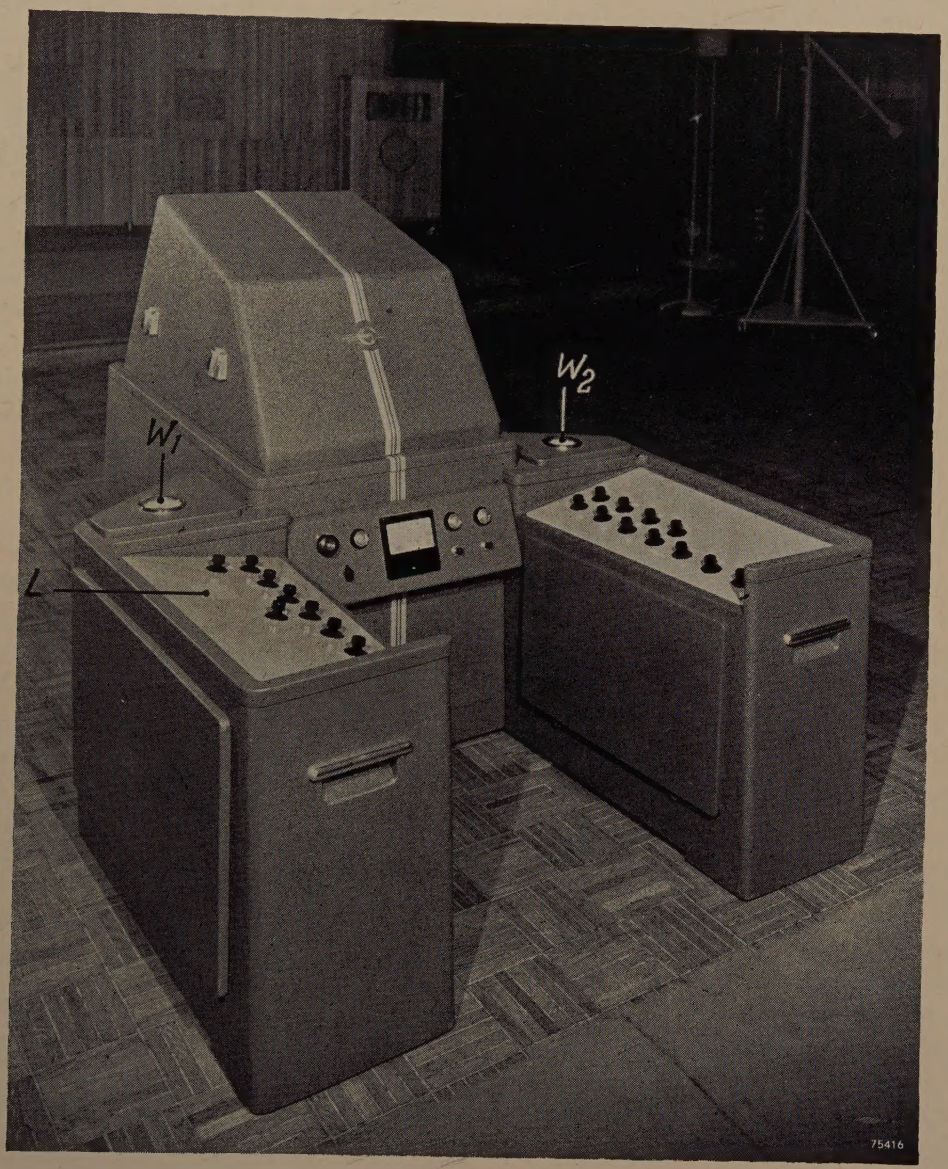

Fig. 6. Rear view of the projector. The left-hand wing contains a television receiver and an A.F. amplifier (25 W); the right-hand wing houses saw-tooth voltage generators for horizontal and vertical deflection, and also a video amplifier. The main body of the unit contains the optical system, H.T. generator and ancillary equipment. The meter indicates the beam current of the projection tube.

L monitor loudspeaker; W_1 and W_2 small cathode-ray tubes (type MW 6-2) for monitoring the picture as from the output of the receiver and video amplifier.

This equipment is complete in itself except for the aerial, the projection screen and the loudspeakers.

As already mentioned above, the distance from he projector to the screen must be 8 m for a magnication of 40×; this is simultaneously the minimum istance from which the audience should view the screen if the lines in the image are not to be perceptible to an uncomfortable degree. This minimum distance is based on the rule of thumb that it should be equal to twice the height of the picture (this rule holds for 625 lines; for other systems the distance is inversely proportional to the number of lines). The front row of the seating accomodation can accordingly be arranged on each side of, or just behind the projector, which has therefore been kept sufficiently low in design to prevent it from obstructing the view of the screen; the overall height of

the unit is not more than 1.15 m (3'-10"). The floor space occupied is only 1.35 × 1.65 m (4'-5" × 5'-5") (*fig. 7*).

As is seen in fig. 3 the upper part of the main body of the projector houses the cathode-ray tube and the optical system. Below these are the generator (fig. 4) and a stabilized rectifier unit for lower voltages. Mounted at the rear, within the immediate reach of the projectionist, is the panel which carries

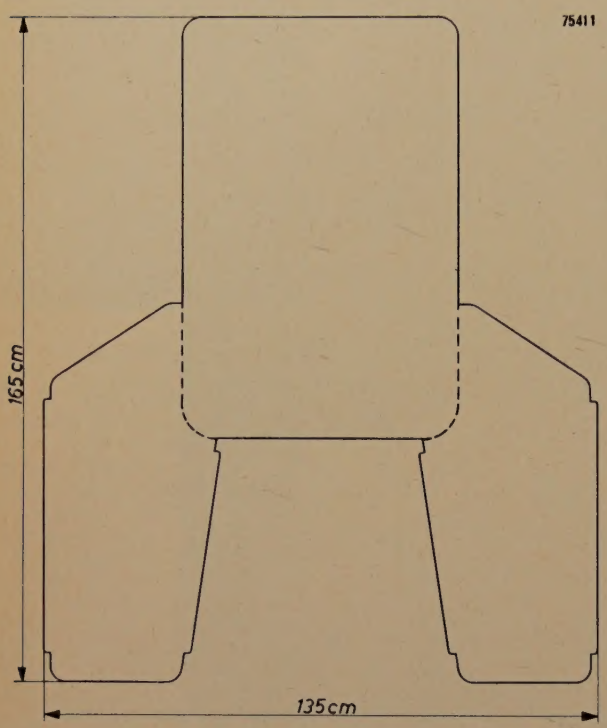

Fig. 7. Plan view of the projector (dimensions in cm). To facilitate transportation the wings can be detached from the main body (at the dotted lines).

the main switch, on/off buttons for the H.T. generator, a meter to indicate the tube current, and several indicator lamps (fig. 6).

The left-hand wing (fig. 6) contains a television receiver and sound amplifier, the latter having an output of 25 W. Both the sound and the picture can be monitored by the projectionist by means of a small loudspeaker and a cathode-ray tube which are also mounted in the left-hand wing.

In the right-hand wing are the video amplifier and the time base generators for the tube, and these also operate a small monitor tube; the projectionist does not switch on the projection tube until he is sure that the image on the monitor tube is satisfactory, particularly as regards synchronisation, thus sparing the audience the sight of confused and imperfectly synchronised images.

The MW 6-2 is used for both monitor tubes, this being the standard tube in projection receivers for home use [13]); in this case it is employed as a direct-vision tube and 9 kV is sufficient to operate it.

The video and A.F. amplifiers can if desired be connected to a television camera and microphone in "closed circuit", instead of to the receivers; the amplifiers are fully loaded for a video signal of 1.5 V across 75 Ω and an audio signal of 0.8 V across 500 Ω (in both cases peak to peak).

Needless to say, the necessary precautions have been taken to prevent contact with live parts of the equipment. For example the opening through which the light is emitted is fitted with a wire guard, so that the hands cannot be inserted. In the event of a fault developing in one of the generators, the beam current of the projection tube is suppressed to avoid damage to the fluorescent screen

The equipment can be easily moved about, as it is fitted with castors. With a view to transportation the wings are easily detachable; the electrical connections are completed by means of plugs and sockets, and the mechanical assembly with bolts and wing nuts. When detached, each of the three parts can be rolled along the floor.

As will be apparent from this description, the equipment as illustrated in figs 5 and 6, is self-contained (with the exception of the aerial, projection screen and loudspeakers).

The acknowledgements of the authors of this article are due to a large circle of co-workers.

[13]) See article II, referred to in footnote [3]).

Summary. A description is given of the "Mammoth" television-projector (type EL 5750), which is capable of giving pictures 4 × 3 m in size with a brightness (luminance) equal to that of cinema pictures (peak, 17 nit). The projector contains a 12 cm cathode-ray tube (type MW 13-16) operating on 50 kV, and a Schmidt optical system (concave spherical mirror with correcting plate). The dissipation at the fluorescent screen of the tube is 25 W and the screen is cooled by a jet of air. All the components, viz. the television receiver, video and A.F. amplifiers and H.T. generator are combined in this equipment, which can be operated by one person. The projector is mounted about 8 m from the projection screen, in front of the audience; it occupies a floor space of 1.35 × 1.65 m and is only 1.15 m in height. All the controls are within easy reach of the projectionist, and two small tubes and a loudspeaker are included for monitoring both picture and sound.

ABSTRACTS OF RECENT SCIENTIFIC PUBLICATIONS OF N.V. PHILIPS' GLOEILAMPENFABRIEKEN

Reprints of these papers not marked with an asterisk * can be obtained free of charge upon application to the address on the back cover.

015: K. H. Klaassens, J. Bakker, C. J. Schoot, J. Goorrissen: A simple method of measuring the moment of disappearance of soap micelles during polymerisation in emulsion (J. Polymer Sci. **7**, 457-461, 1951, No. 5).

A simple method is described for determining the ıoment of disappearance of soap micelles during he emulsion polymerisation of styrene by measurıg the electrolytic conductivity during the polyıerisation (with the potassium salt of stearic acid s a soap and potassium persulfate as an initiator). 'he results have been verified using the method of ırface tension.

It is generally assumed that in the initial stages f an emulsion polymerisation soap in the aqueous hase is largely present in the form of soap micelles ut rapidly transforms into monolayers surrounding he polymer-monomer particles formed by the olymerisation reaction.

016: H. Bremmer: The jumps of discontinuous solutions of the wave equation (Comm. pure and appl. Math. **4**, 419-426, 1951, No. 4).

The connections existing between steady-state olutions and pulse solutions (in Luneberg's sence) f Maxwell's equations are studied. Luneberg's heory is based on the integration of Maxwell's quations over four-dimensional space-time domains. 'he present simplification of this theory is based on he use of the Heaviside unit function and the)irac delta function. Equations for the eiconal ınction and for discontinuities on wave fronts in calar wave propagation are treated in detail.

017: E. J. W. Verwey, P. B. Braun, E. W. Gorter, F. C. Romeijn, J. H. van Santen: Die Verteilung der Metallionen im Spinellgitter und deren Einfluß auf die physikalischen Eigenschaften (Z. phys. Chem. **198**, 6-22, Oct. 1951). (The distribution of metallic ions in the spinel lattice and its influence on the physical properties; in German.)

After dealing with the distribution of the cation istributions in several oxygen spinels, as deterıined by X-ray analysis; the cases in which normal r inverted spinels are to be expected are discussed, using a heteropolar model. In the case of inverted spinels special attention is paid to the problem of order. The electrical problems of the ferrite spinels are in agreement with a theory exposed in anterior publications. The difference between Fe_3O_4 and Mn_3O_4 is discussed. The ferromagnetic saturation of the simple ferrites and their mixed crystals with zinc ferrite can be explained from Néel's theory. The indirect exchange interaction between magnetic ions is discussed. The influence of the angle Fe-O-Fe and its variation are in qualitative agreement with Anderson's theory. See Philips tech. Rev. **9**, 185-190, 231-248, 1947-48 and **13**, 194-208, 1952, No. 7.

2018: C. J. Schoot, J. Bakker and K. H. Klaassens: Remark on the article by S. R. Shunmickham, V. C. Hallenbeek and R. L. Guile, "Emulsion polymerisation of styrene, II. Effect of agitation" (J. Polymer Sci. **7**, 657, 1951, No. 6).

The effect of agitation on emulsion polymerisation, as found by Shunmickham and others, is ascribed to contamination of the nitrogen gas used in the experiments with traces of oxygen.

2019: H. P. J. Wijn and J. J. Went: The magnetisation process in ferrites (Physica **17**, 976-992, 1951, No. 11/12).

Initial magnetization curves of ferrites have been measured as a function of frequency up to 2 Mc/s. It has been found that the magnetization of sintered ceramic ferrites with a high permeability is brought about by at least two processes, one of which, in the frequency range covered, is independent of frequency and determines the initial permeability. The other process has a relaxation frequency of about 200 kc/s and is responsible for the irreversible processes during magnetization. From measurements on samples of sintered ferrites fired at different temperatures, it has been concluded that the frequency-dependent magnetization is caused by irreversible Bloch-wall displacements, whilst the initial permeability is caused by a reversible rotation of the magnetization in Weiss domains in the direction of the external magnetic field (in contrast to what is believed to be the case in cast ferromagnetic metals). A discussion shows that neither eddy current effects nor any inertia effects

so far known are responsible for the relaxation frequency of the Bloch wall at about 200 kc/s.

2020: M. E. Wise: Free electrons, traps and glow in crystal phosphors (Physica **17**, 1011-1032, 1951, No. 11/12).

The well known monomolecular and bimolecular theories of afterglow and thermal glow are summarized. Observed results on phosphors of ZnS type are discussed, particularly the phosphors with long afterglow in which the intensity-time laws are hyperbolic. These have been explained by many workers in this field by a monomolecular theory with a distribution of depths of electron traps. It is shown that certain mathematical approximations that must be used in relating the theory to observations of afterglow and thermal glow are not sufficiently accurate. A new and simple law is given that describes the same observations more exactly. A new physical theory for the free and trapped electrons is outlined, and this is discussed in relation to F and F′ centres in alkali halides and to an unsolved problem of semi-conductor theory.

R 179: J. L. H. Jonker: On the theory of secondary electron emission (Philips Res. Rep. 7, 1-20, 1952, No. 1).

Starting from (1) Whiddington's law concerning the velocity loss of electrons penetrating into a solid substance, (2) the experimental absorption law and (3) the assumption that the distribution of the secondary electrons within matter is isotropic, the author calculates the behaviour of secondary electrons as a function of various parameters. Good agreement is found with results obtained experimentally.

R 180: J. Volger: The specific heat of barium titanate between 100 °K and 410 °K (Philips Res. Rep. 7, 21-27, 1952, No. 1).

The specific heat of polycrystalline $BaTiO_3$ has been measured in a Nernst calorimeter. The lattice contribution cannot be described accurately with a single Debye function. In three transition regions the anomalous peaks in the specific heat have been determined.

R 181: W. J. van de Lindt: Application of multi-hole coupling to the design of a variable and calibrated waveguide attenuator and impedance (Philips Res. Rep. 7, 28-35, 1952, No. 1).

A short introduction describes the behaviour of two parallel waveguides, mutually coupled by n equidistant identical directional elements. A new type of calibrated variable attenuator and a variable impedance, capable of changing independently the amplitude and the phase of the reflection coefficient, are discussed.

R 182: G. Diemer and K. Rodenhuis: Optimum geometry of microwave amplifier valves (Philips Res. Rep. 7, 36-44, 1952, No. 1).

On the basis of Van der Ziel and Knol's theory of feedback amplifiers it is shown that for u.h.f. amplifier valves the maximum frequency limit for the amplification is reached if the electrode areas are so chosen that the useful capacitance is equal to the unavoidable stray capacitance. For optimum value of the product (gain × bandwidth), the useful capacitance should be somewhat higher.

R 183: G. Diemer and H. Dijkgraaf: Langmuir's ξ, η tables for the exponential region of the I_a-V_a characteristic (Philips Res. Rep. 7, 45-53, 1952, No. 1).

The inter-electrode distances of modern microwave diodes and triodes are often so small that the normal operating point lies in the exponential part of the characteristic. A set of ξ,η tables with the voltage gradient at the anode as parameter is given, from which the potential distributions in such cases can be derived. (See **R 7** and **R 8.**)

R 184: J. B. de Boer, V. Oñate and A. Oostrijck: Practical methods for measuring and calculating the luminance of road surfaces (Philips Res. Rep. 7, 54-76, 1952, No. 1).

In defining the qualities of an installation for road illumination the luminance distribution of the road surface is a more important factor than the illumination. However, owing to the lack of precise and quick methods of measuring and computing luminance, illumination values have mainly been used. In this paper methods are described which now enable the public lighting engineer to use road luminance in practice. The reflection properties of one particular road surface (dry asphalt) have been measured. Finally an example of the calculation of luminance is given in the appendix.